Shortcut Methods for Nonideal Multicomponent Distillation: 3. Extractive Distillation Columns

Stefan Brüggemann and Wolfgang Marquardt
Lehrstuhl für Prozesstechnik, Rheinisch–Westfälischen Technische Hochschule (RWTH) Aachen, D-52056 Aachen, Germany

DOI 10.1002/aic.10108
Published online in Wiley InterScience (www.interscience.wiley.com).

Extractive distillation is a common process for the separation of homogeneous azeotropic mixtures with a minimum boiling azeotrope. In this process entrainer feed flow rate and reflux ratio of the extractive column represent the crucial design degrees of freedom that govern feasibility and operating cost. In this work feasibility and operational stability of the extractive column are related to the nonlinear analysis of the extractive section. A fully automated conceptual shortcut design method for the simultaneous determination of minimum entrainer feed flow rate and minimum reflux ratio is presented. The method is applicable to arbitrary multicomponent mixtures and allows direct screening of design alternatives and comparison of different entrainers. © 2004 American Institute of Chemical Engineers *AIChE J,* 50: 1129–1149, 2004
Keywords: multicomponent extractive distillation, minimum energy demand, rectification body method (RBM), economic screening, entrainer selection

Introduction

Extractive distillation is commonly used to separate mixtures that display minimum boiling azeotropes. In the extractive column a heavy boiling entrainer is fed to a tray above the main feed stream. The entrainer facilitates the separation by interacting with the azeotropic mixture and altering the thermodynamic equilibrium in the extractive section of the column. Figure 1 displays the column configuration for a binary process feed. The heavy entrainer E preferably associates to component B and takes it down the column. Therefore a binary mixture of B and E is recovered in the bottom product, whereas high-purity A is obtained in the distillate product. Separation feasibility and process cost are characterized by two major parameters, the entrainer feed flow rate and the reflux ratio (or condenser and reboiler heat duties; see shaded degrees of freedom in Figure 1). In addition to minimum reflux, which limits feasibility for all zeotropic and azeotropic separations, there is a maximum reflux for extractive distillation above which separation cannot be achieved. These bounds for the reflux ratio depend on the entrainer feed flow rate. The range of feasible choices for the reflux ratio decreases with decreasing entrainer flow rates. Below a minimum entrainer flow rate the extractive effect is no longer sufficient for separation and a feasible reflux policy cannot be found (Andersen et al., 1995).

The standard approach for process design of such separation processes usually involves the detailed specification of all relevant design parameters, for example, the number of trays, the location of process and entrainer feed trays, the entrainer flow rate, and the reflux ratio (or either condenser or reboiler heat duty; see Figure 1). This column configuration is analyzed using a standard process simulator such as Aspen+ or HYSYS. The design engineer is left with the difficult task to iteratively change the design variables and repeat this process until all design constraints (such as required purities, and so on) are met and convergence is achieved. Such simulation-based design is a good method to specify all relevant design variables, although it is also a rather tedious and time-consuming undertaking.

In the early stages of process synthesis a large number of different design alternatives can be formulated. A good example is the purification of a binary alcohol–water mixture, which can be achieved by heteroazeotropic distillation using a heterogeneous entrainer (Pham et al., 1989; Urdaneta et al., 2002),

Correspondence concerning this article should be addressed to W. Marquardt at marquardt@lpt.rwth-aachen.de.

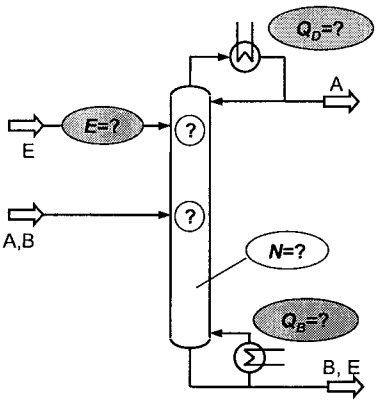

Figure 1. Design degrees of freedom of the extractive column.

extractive distillation using a homogeneous entrainer (Black, 1980), or by using a hybrid membrane-distillation configuration (Bausa and Marquardt, 2000). For both the homogeneous and the heterogeneous azeotropic distillation processes the choice of the entrainer, usually from a list of potential candidates, defines the structure of the process and is crucial to the economic performance. For example, such lists of entrainer candidates may be obtained by a search of the literature or by computer-aided molecular design (CAMD; Harper et al., 1999). The number of structurally different design alternatives then easily grows too large to be effectively tackled using simulation tools. Therefore, there is a need for simple and fast algorithms that support process screening and provide an estimate of economic potential. For such rough economic screening it is often sufficient to reduce the economic evaluation to the energy demand of the separation. Then the conceptual design task can be confined to finding an entrainer flow rate and a reflux ratio (or heat duties; see shaded degrees of freedom in Figure 1) such that the operation of the column is both feasible and economically attractive. In the following sections the term *column design* will be restricted to this definition of conceptual design.

Shortcut methods for the assessment of the feasibility of a separation and determination of the minimum energy demand of distillation are well suited for such design tasks because they allow fast evaluation of the separation without needing detailed unit information and present valuable insight into the thermodynamic limitations of the mixture. For the separation of ideal mixtures the shortcut method of Underwood (1948) has become a standard tool for process design. In the last 20 years several research groups have proposed geometric criteria for the determination of the minimum energy demand of nonideal distillation. The first article of this series (Bausa et al., 1998) presents a critical review of state-of-the-art methods and the authors propose a new, entirely general method for the separation of arbitrary nonideal multicomponent mixtures in single-feed columns. For extractive distillation in columns with two feed streams a general design method is missing. In this work feasibility and operability of extractive columns will be related to the pinch topology of the extractive section, which is obtained from nonlinear analysis. It will be shown that a lower bound for the entrainer feed as well as a lower and an upper bound for the reflux ratio can be directly obtained from a bifurcation analysis of the pinch map of this section. The shortcut method of Bausa et al. (1998) is extended for columns with two feed streams. Bifurcation analysis and the shortcut method are then combined to form a new design method for extractive distillation processes that is entirely general, applicable for an arbitrary number of components, and can be fully automated. The results of this shortcut design algorithm can be used to directly compare the economic performance of different entrainers and provide good initial values for more rigorous calculations such as mixed-integer nonlinear optimization (MINLP; Bauer and Stichlmair, 1998).

Nonlinear Analysis of Extractive Distillation

In the last 20 years several research groups have investigated the behavior of extractive distillation processes. Most of the publications focus on the analysis of the middle section of the column between the upper extractive and the lower process feed because the manipulation of the thermodynamic equilibrium by injection of the extractive agent overcomes the limitations for the product purities imposed by the azeotrope. In this section some important properties of the extractive column section will be reviewed. To illustrate these properties a simple ternary example, the separation of an azeotropic mixture of isopropanol and water using pure ethylene glycol as the heavy entrainer, will be introduced.

Illustrative separation example

The thermodynamic behavior of ternary mixtures can be visualized using residue curve maps, which represent the composition profiles of a simple batch still or of a column operating at infinite reflux. Doherty and Caldarola (1985) identified all classes of ternary residue curve maps that allow separation using extractive distillation processes. Therefore all feasible entrainers must give rise to one of these residue curve topologies. Foucher et al. (1991) simplified this residue curve analysis and present an algorithm for checking the feasibility of an entrainer that can easily be automated. Figure 2 shows the residue curve map for the isopropanol–water–ethylene glycol (PWG) example. The topology of this mixture is typical for extractive distillation processes. All profiles originate from the

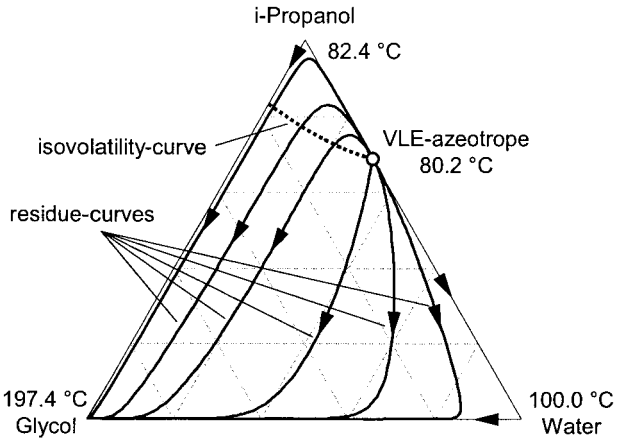

Figure 2. Residue curve map and isovolatility curve for the PWG separation.

minimum boiling azeotrope, which is the unstable node of the residue curve map, and end at the pure ethylene glycol vertex, which corresponds to the stable node of the residue curve diagram. Profiles running close to the edges of the composition space are attracted either by the pure isopropanol or pure water vertices and then repelled toward the stable node (that is, the glycol vertex). In the context of nonlinear analysis the isopropanol and water vertices thus correspond to saddle points of the residue curve map. Mathematically all these nodes and saddles are fixed points of the residue curve map. It is important to note that these fixed points completely describe the qualitative behavior of all packed-column profiles at infinite reflux (Doherty and Perkins, 1978).

Another interesting piece of information can be obtained from the isovolatility curve of isopropanol and water (see Figure 2), which can be calculated from

$$\frac{y_P/y_W}{x_P/x_W} = \frac{K_P}{K_W} = 1. \tag{1}$$

Laroche et al. (1991) show that the component that can be withdrawn with high purity from the extractive column in the distillate product can be directly determined from an analysis of the isovolatility curves. The fundamental behavior of an extractive column requires a change in the local volatility order along the binary axis of the distillate component and the entrainer (that is, intersection between the isovolatility curve and this binary axis). In the PWG example the distillate will therefore be specified as high-purity isopropanol. Using this information and assuming that the bottom product will be essentially free of isopropanol, the distillate flow rate can be calculated from the mass balance around the column. In fact, the only information missing to completely specify all input and output streams is the entrainer feed flow rate.

Column behavior at finite reflux

Although the fixed points of the residue curve map are sufficient to describe column profiles at infinite reflux, they do not represent the course of profiles at finite reflux. Nonlinear analysis, however, can also be applied to columns with finite reflux by augmenting the thermodynamic equilibrium equations with the material and heat balances around each tray. The occurrence of a fixed point implies that all state variables (i.e., concentrations and internal flow rates) do not change from one tray to the next. The set of equations defining these fixed points is

$$V - L - N = 0, \tag{2}$$

$$Vy_i - Lx_i - Nx_{N,i} = 0, \qquad i = 1, \ldots, C, \tag{3}$$

$$y_i - K_i x_i = 0, \qquad i = 1, \ldots, C, \tag{4}$$

$$\sum_{j=1}^{C} (y_j - x_j) = 0, \tag{5}$$

$$Vh^V - Lh^L - Nh_N = 0, \tag{6}$$

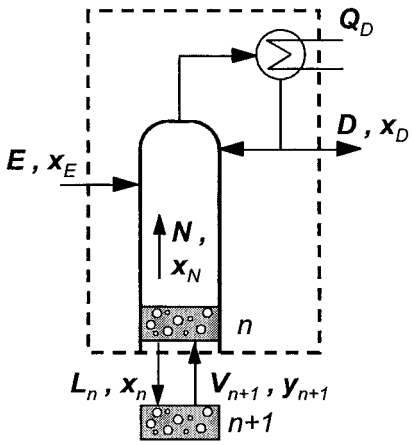

Figure 3. Balance envelope of the extractive section.

where N, $\mathbf{x}_N$, and h_N describe the net stream into a column section from below. For the extractive middle section of the column (see Figure 3) these quantities are defined as

$$N = D - E, \tag{7}$$

$$Nx_{N,i} = Dx_{D,i} - Ex_{E,i}, \qquad i = 1, \ldots, C, \tag{8}$$

$$Nh_N = Dh_D - Eh_E + (r + 1)\, D\Delta h^{VAP}(\mathbf{x}_D). \tag{9}$$

The vapor–liquid distribution coefficients K_i and the enthalpies h^L and h^V are functions of the compositions, temperature, and pressure:

$$K_i = f(\mathbf{x}^T, \mathbf{y}^T, T, p), \qquad i = 1, \ldots, C, \tag{10}$$

$$h^L = f(\mathbf{x}^T, T, p), \qquad i = 1, \ldots, C, \tag{11}$$

$$h^V = f(\mathbf{y}^T, T, p), \qquad i = 1, \ldots, C. \tag{12}$$

By inserting Eqs. 7–9 and the physical property correlations 10–12 into the set of fixed point Eqs. 2–6, we obtain a system of $3 + 2C$ equations with $6 + 4C$ variables $\mathbf{x}$, $\mathbf{y}$, T, V, L, r, D, $\mathbf{x}_D$, E, and $\mathbf{x}_E$. Assuming a fixed entrainer composition $\mathbf{x}_E$ and using the specifications of the separation from the isovolatility analysis, the set of variables can be partitioned into the fixed problem-specific design specifications $\boldsymbol{\varphi} = (\mathbf{x}_D^T, D, \mathbf{x}_E^T)^T$, the dependent variables $\mathbf{u} = (\mathbf{x}^T, \mathbf{y}^T, T, V, L)^T$, and the design degrees of freedom r, E. The set of Eqs. 2–6 can then be abbreviated as

$$\mathbf{f}(\mathbf{u}, \boldsymbol{\varphi}, r, E) = \mathbf{0} \tag{13}$$

which is commonly known as the *pinch equations*. Their solutions are referred to as *pinch points*. Choosing a fixed value for the entrainer flow rate E the solutions of Eqs. 2–6 are one-dimensional functions of the reflux ratio r and the loci of these solutions are called *pinch branches*. These pinch branches can be calculated by homotopy continuation (for details, see Bausa, 2001).

Figure 4a shows the pinch branches as a function of the

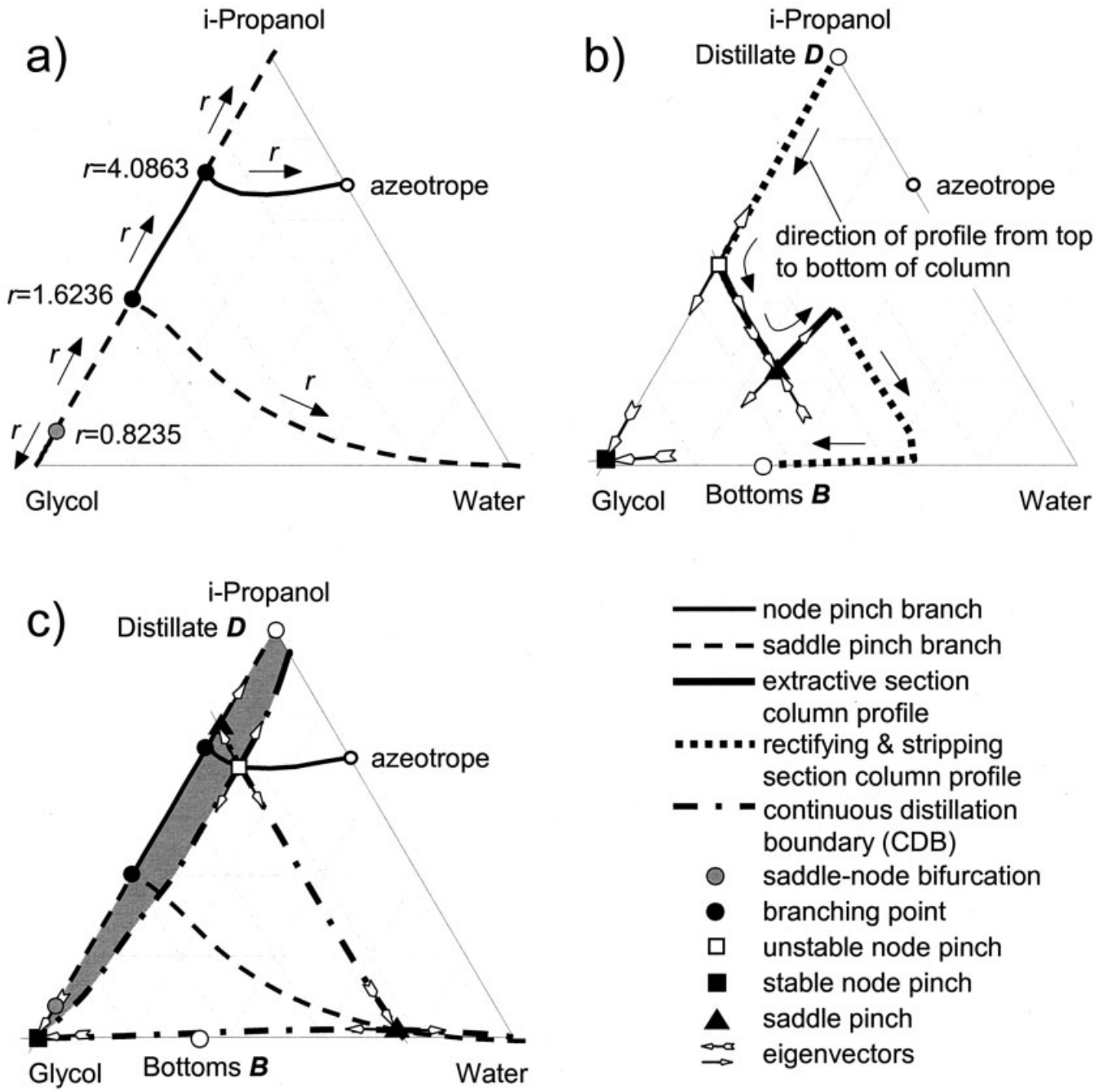

Figure 4. Extractive section of PWG separation at a fixed entrainer-to-feed ratio of $E/F = 0.750$.

(a) Bifurcation diagram of pinch points as a function of r. (b) Pinch points, eigendirections, and feasible column profile for $r = 2.042$. (c) Pinch points for an infeasible separation at $r = 5.0$ and continuous distillation boundaries.

reflux ratio r for a fixed entrainer to process feed ratio of $E/F = 0.750$. The pinch points for a reflux ratio of $r = 2.042$ and the column profile obtained from an Aspen+ simulation with the same specifications and a large number of trays are presented in Figure 4b. It can be seen that there are two types of pinch branches that connect the azeotrope and all pure component vertices. The type of the pinch branch, node or saddle, depends on the stability of the pinch points located on it. The stability and the directions from which a column profile either approaches the pinch or is repelled from it can be determined using the eigenvalues and eigenvectors at the pinch (for details, see Bausa, 2001; Julka and Doherty, 1990). For the given reflux three pinch points, an unstable node on the isopropanol-glycol edge, a stable node close to the glycol vertex, and a ternary saddle are found. Comparing the extractive section column profile in Figure 4b with the pinch points and their eigendirections it can be seen that the pinch points and the associated eigendirections give a good qualitative approximation of the column profile in this section. Moreover, the existence of the ternary saddle pinch is obviously an important

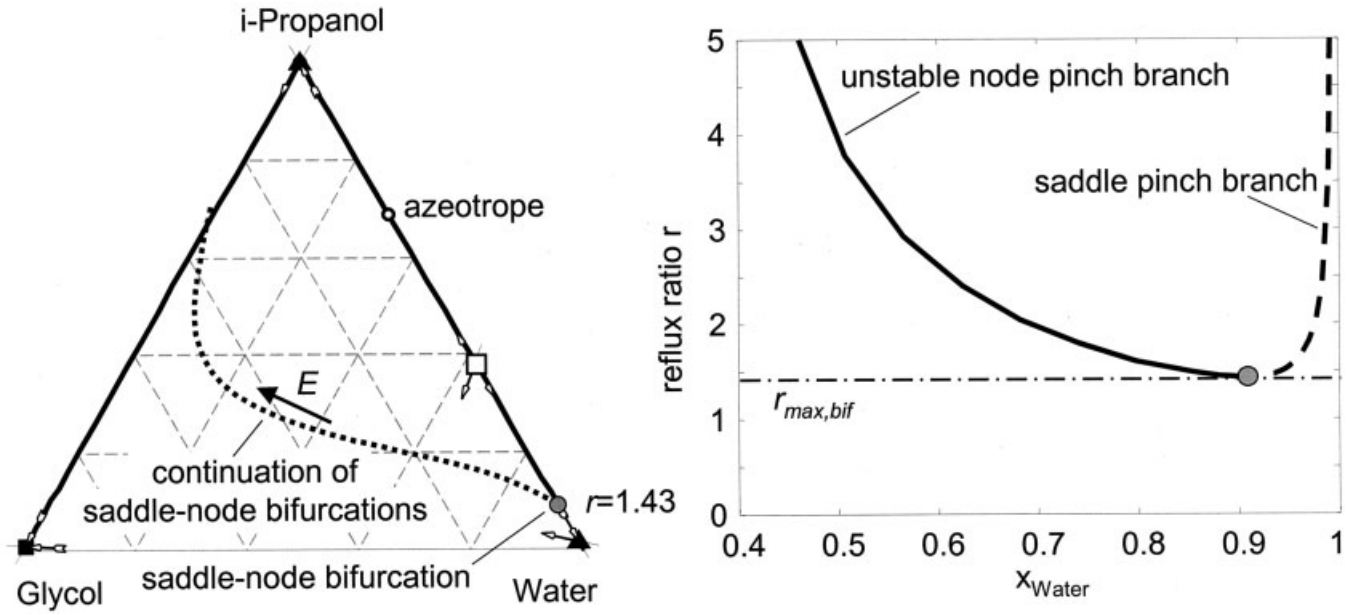

Figure 5. Pinch branches (solid, dashed) at $E/F = 0$, pinch points at $r = 3.0$ and locus of saddle-node bifurcation (dotted) for $E \geq 0$ (left); reflux ratio along the pinch branch on the propanol–water edge (right).

Refer to Figure 4 for a legend on the pinch points, bifurcation points, and the eigenvectors.

factor for the connection of the rectifying and stripping section column profiles (dotted lines) by the extractive section column profile (continuous line).

Figure 4c shows the pinch branches and specific pinch points for the same entrainer feed flow rate but a larger reflux ratio $r = 5.0$. The pinch points have moved on their respective branches according to the higher energy supply to the column. The unstable node pinch has moved from the isopropanol–glycol edge [cf. Figure 4b] into the ternary space; the saddle pinch has moved toward the glycol-water edge; and a new saddle pinch has appeared on the binary isopropanol–glycol edge. A simulation with Aspen+ shows that the desired product specifications cannot be obtained for this reflux. Careful examination of Figure 4c leads one to draw this conclusion directly from the pinch diagram. Because of the occurrence of the ternary unstable node on the pinch branch originating at the azeotrope there can be no extractive section profile that connects the rectifying section to the stripping section profile as in Figure 4b.

Fidkowski et al. (1993) introduce the concept of continuous distillation boundaries (CDB) that easily provides an illustration of this situation. The CDB [chain dotted lines in Figure 4c] cannot be crossed by feasible column profiles and therefore confine all feasible profiles into self-contained regions of the composition space. In the PWG example all column profiles, starting from the binary isopropanol–glycol edge where the rectifying profile is located, will stay close to this binary edge in the shaded region and cannot access the stripping profile, which lies in a different distillation region.

By comparing Figure 4b and 4c, it can be concluded that the appearance of the ternary unstable node on the pinch branch originating at the azeotrope makes the separation infeasible, whereas the existence of a ternary saddle originating from a pure component is a prerequisite for a feasible process. Knapp and Doherty (1994) formulate this criterion and relate separation feasibility to the appearance of saddle-node bifurcation points and branching points. Saddle-node bifurcation points are extremal points of the pinch branch with respect to the reflux ratio. Their appearance results in a change of stability of the pinch branch, for example, from a saddle to a stable node pinch branch [cf. gray circle in Figure 4a]. Branching points are found where two pinch branches intersect [cf. black circles on the binary isopropanol/glycol edge in Figure 4a]. Such a branching point corresponds to saddle-node behavior and therefore a change in stability on both intersecting pinch branches. To illustrate these bifurcation phenomena the effect of the entrainer to process feed ratio on the course of the pinch branches will be discussed first.

Nonlinear analysis of pinch equations

Figure 5 shows the pinch branches when no entrainer is added to the column. At $r = 3.0$ four pinch points are found. Note that these pinch points at finite reflux can be directly deduced from the fixed points of the residue curve map (cf. Figure 2) because the fixed points of the residue curve map are identical to the pinch points at infinite reflux. The pinch points at finite reflux are obtained by slowly decreasing the reflux ratio and observing the movement of the fixed points. Therefore the four pinches displayed in Figure 5 for $r = 3.0$ can be related to the three pure components and the azeotrope. Glycol is the heaviest species of this mixture and therefore corresponds to a stable node pinch. Regarding the azeotrope as a pseudocomponent, isopropanol and water are intermediate boilers and therefore correspond to saddle pinches. The azeotrope is the lightest component and therefore corresponds to an unstable node. Because of the finite reflux the unstable node pinch has moved, however, from the azeotrope on its pinch branch toward the water vertex. Keeping in mind that the appearance of an unstable node pinch on the azeotrope pinch branch is a crucial factor for split feasibility in extractive

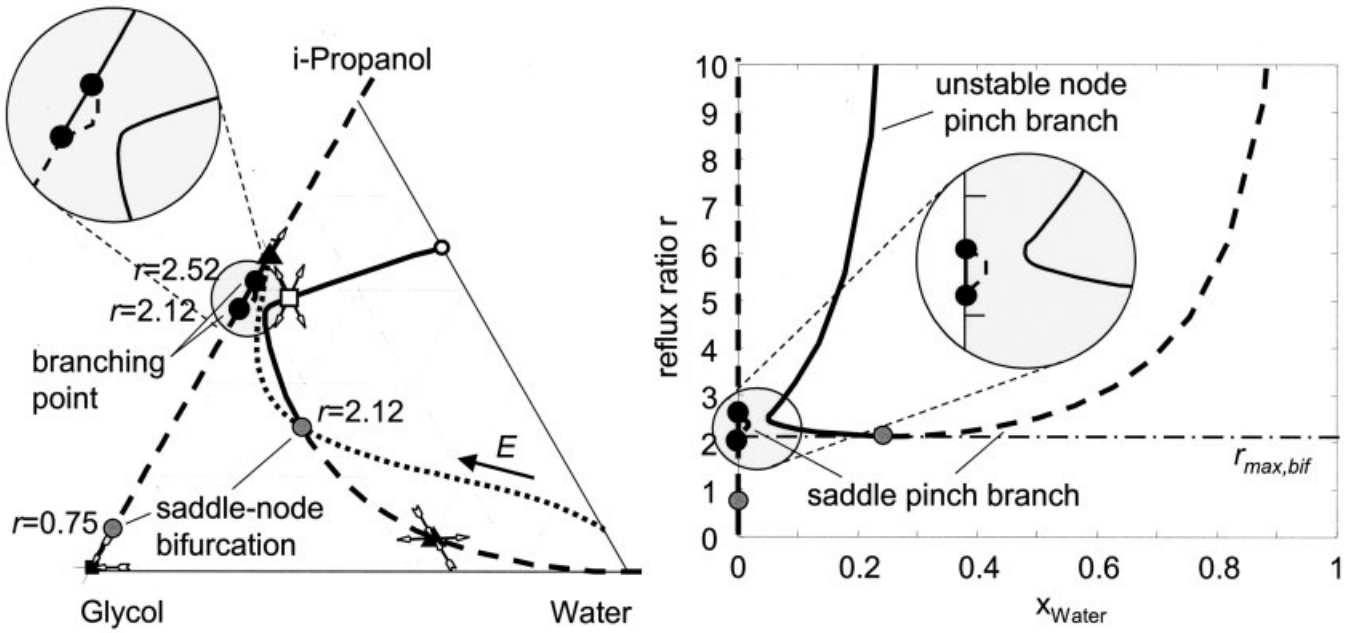

Figure 6. Pinch branches (solid, dashed) and branching points at $E/F = 0.648$, pinch points at $r = 3.0$ and locus of saddle-node bifurcation (dotted) for $E \geq 0$ (left); reflux ratio along the pinch branches (right).

Refer to Figure 4 for a legend on the pinch points, bifurcation points, and the eigenvectors.

distillation, this unstable node and its pinch branch deserve further attention. Figure 5 (right) shows the reflux ratio r along the pinch branch on the binary isopropanol–water edge as a function of x_W. For infinite reflux the unstable node and the saddle branch originate at the azeotrope and at the pure water vertex, respectively. For decreasing reflux the pinch points approach each other until they meet and are extinguished in a saddle-node bifurcation point at $r = r_{max,bif} = 1.43$. Because of the appearance of the unstable node pinch, the binary separation of isopropanol and water is not feasible for $r \geq r_{max,bif}$. For $r < r_{max,bif}$ the unstable node pinch that prohibits separation on the isopropanol–water edge no longer exists. However, it can already be inferred from the binary azeotrope that a feasible separation can never be achieved. Therefore, the extractive effect of the entrainer is needed.

A saddle-node bifurcation is an extremal point of the pinch branch with respect to the reflux ratio. Close to a saddle-node bifurcation the Jacobian of the pinch equations becomes singular and the exact location of the saddle-node bifurcation can therefore be obtained from

$$\mathbf{f}(\mathbf{u}, \varphi, r, E) = \mathbf{0}, \tag{14}$$

$$\nabla_{\mathbf{u}}\mathbf{f}(\mathbf{u}, \varphi, r, E)\mathbf{w} = \mathbf{0}, \tag{15}$$

$$\mathbf{w}^T\mathbf{w} - 1 = 0, \tag{16}$$

where $\mathbf{w}$ is a null vector of $\nabla_{\mathbf{u}}\mathbf{f}(\mathbf{u})$ (Beyn et al., 2002). Given a value of E, the system of Eqs. 14–16 can readily be solved with a Newton method for $\mathbf{u}$, $\mathbf{w}$, and r if good initial guesses are known. Here, the local minimum of the of the pinch branch continuation with respect to the reflux ratio r provides a good initial guess for $\mathbf{u}$ and then $\mathbf{w}$ is initialized with the eigenvector corresponding to the smallest eigenvalue of $\nabla_{\mathbf{u}}\mathbf{f}(\mathbf{u})$. The location of all saddle-node bifurcations is obviously a one-dimensional function of the entrainer flow rate E. Hence, the loci of all saddle-node bifurcation points can be determined analogously to the calculation of pinch branches by applying homotopy continuation to Eqs. 14–16. The resulting saddle-node bifurcation branch, starting from the unstable node pinch on the azeotrope pinch branch, is shown in Figure 5 (left).

Figure 6 (left) shows the bifurcation diagram for the pinch loci of the extractive column section for an entrainer to process feed flow rate ratio of $E/F = 0.648$. Pinch points are marked for $r = 3.0$. Because of the introduction of the upper entrainer feed, the azeotrope pinch branch detaches from the binary isopropanol–water edge and moves into the ternary region. Analogously the saddle-node bifurcation of this pinch branch changes its location on the saddle-node bifurcation path. Although the course of the pinch branches and the location of the pinch points and the saddle-node bifurcation change considerably from Figure 5 to Figure 6, the argumentation on the feasibility of the separation remains the same. For reflux ratios larger than the saddle-node bifurcation reflux $r_{max,bif} = 2.12$ a ternary unstable node pinch as well as a ternary saddle are obtained. For reflux ratios below this value no ternary pinch exists. It is thus impossible to fulfill the criterion for feasible separation of Knapp and Doherty (1994) presented above. Note however, that the azeotrope pinch branch approaches the isopropanol–glycol edge for increasing entrainer feed flow rates. Additionally, Figure 6 shows the appearance of a small new saddle pinch branch close to the isopropanol–glycol edge that comes very close to the azeotrope pinch branch (see Figure 6, cutouts).

For a further increase of the entrainer-to-feed flow rate ratio to $E/F = 0.675$, the pinch branches and pinch points shown in

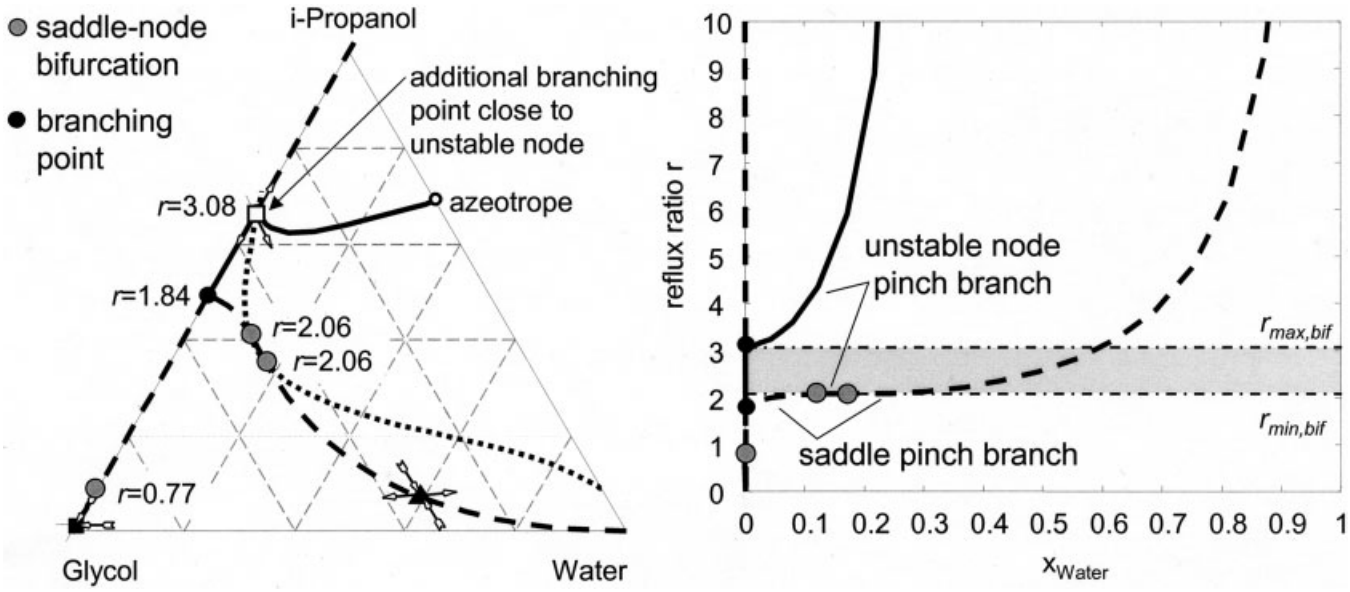

Figure 7. Pinch branches (solid, dashed) and branching points at $E/F = 0.675$, pinch points at $r = 3.0$ and locus of saddle-node bifurcation (dotted) for $E \geq 0$ (left); reflux ratio along the pinch branches (right).

Refer to Figure 4 for a legend on the pinch points, bifurcation points, and the eigenvectors.

Figure 7 are obtained. Although the increase of the entrainer feed flow rate $\Delta(E/F) = 0.027$ from Figure 6 to Figure 7 is relatively small, the topology of the pinch map has changed dramatically. The azeotrope pinch branch is no longer connected to the pure water vertex but instead branches after reaching the isopropanol–glycol edge. The saddle pinch branch originating at the pure water vertex is connected to a second branching point on the isopropanol–glycol edge. Therefore the determination of a ternary saddle pinch on the pinch branch starting at the water vertex is no longer coupled to the simultaneous appearance of a ternary unstable node on the pinch branch originating at the azeotrope. By examining the reflux ratios along the pinch branches (Figure 7, right) it can be seen that there now exists a range of reflux ratios between $r_{min,bif}$ and $r_{max,bif}$, where a ternary saddle can be obtained without the appearance of a ternary node pinch. Within this range the separation is topologically feasible.

Determination of a lower bound for the entrainer flow rate

Knapp and Doherty (1994) present the bifurcation phenomenon that causes the change in topology between $E/F = 0.648$ and $E/F = 0.675$. Revisiting Figure 6 (left), it can be seen that the azeotrope pinch branch and the small pinch branch originating from the branching points on the isopropanol–glycol edge are close to each other. If E/F is increased, they continue to approach each other until they finally intersect at a ternary branching point for $E/F = 0.64894$. Figure 8 shows the corresponding pinch map. Knapp and Doherty (1994) identify this branching point as a pitchfork bifurcation. After the appearance of this pitchfork bifurcation, the pinch branches, starting from the azeotrope and the water vertex, are decoupled. Above the entrainer feed flow rate of the branching point, the separation is topologically feasible. However, the size of the range of feasible reflux ratios is negligible close to this point, and thus $r_{max,bif} \approx r_{min,bif}$.

The pitchfork bifurcation is a codimension-2 singularity in the reflux ratio of parameters r and entrainer-to-feed ratio (E/F). According to bifurcation theory (Beyn et al., 2002) such pitchfork bifurcation marks an extremal point of the state variables with respect to both bifurcation parameters. It can be visualized by plotting one state variable against the two bifurcation parameters. Figure 9 shows such a plot where the liquid mole fraction of water x_W is chosen as the state variable. This is the same choice for the state variable as in Figures 5–8 and thus Figures 5–8 represent two-dimensional (2-D) slices of Figure 9. For $E/F = 0$, the situation is the same as in Figure 5. The unstable node and the saddle pinch branches intersect in a saddle-node bifurcation point. Tracing this saddle-node bifurcation point for increasing entrainer feed ratios using Eqs. 14–16 yields the saddle-node bifurcation branch that marks a minimum of the state variables with respect to the reflux ratio r. The pitchfork bifurcation is found at $(E/F) = 0.64894$ and $r = 2.43$. Close inspection of the graph shows that this point is indeed an extremum for the state variable x_W with respect to both r and E/F.

The pitchfork bifurcation, which marks a ternary branching point of the pinch curves (cf. Figure 8), constitutes a solution to the saddle-node equation system 14–16 and therefore must be located on the saddle-node bifurcation branch. This can also be inferred from Figure 8 (left), given that the stability on each pinch branch changes at the ternary branching point. Figure 10 shows the reflux ratio r on the saddle-node bifurcation branch as a function of the entrainer-to-feed ratio E/F resulting from a homotopy solution of Eqs. 14–16 with respect to E. The pitchfork bifurcation point corresponds to a local minimum of this curve with respect to r. Therefore, the entrainer flow rate

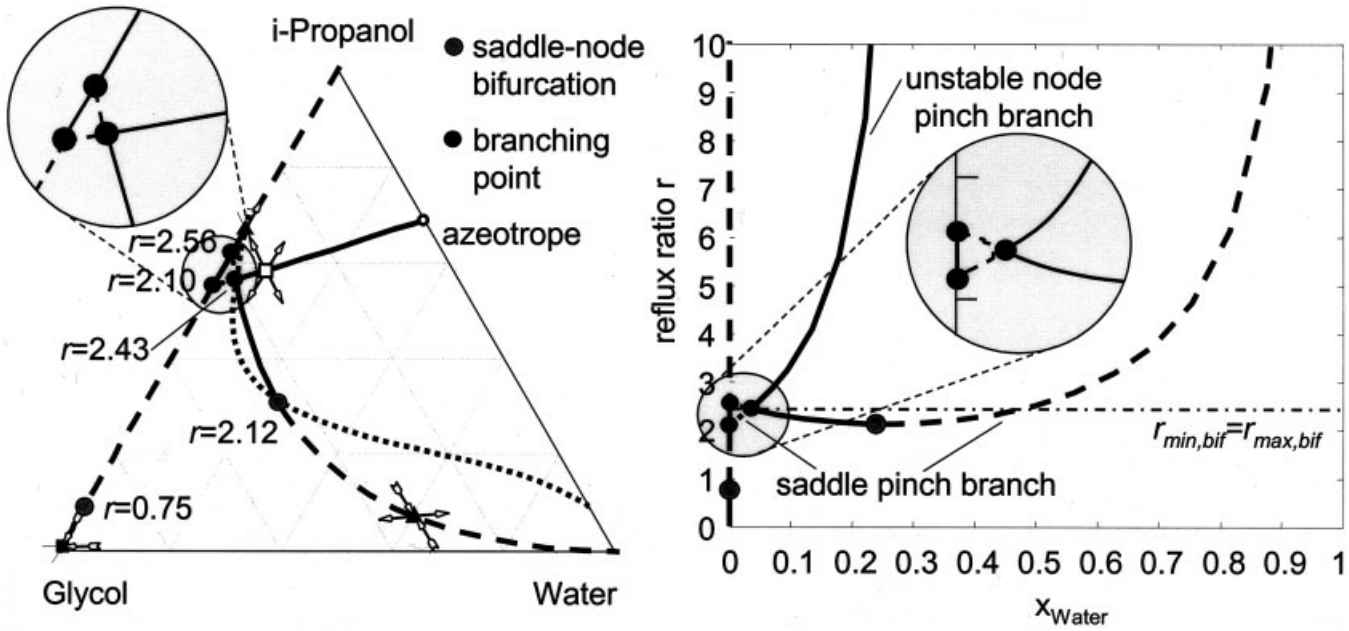

Figure 8. Pinch branches (solid, dashed) and branching points at $E/F = 0.64894$, pinch points at $r = 3.0$ and locus of saddle-node bifurcation (dotted) for $E \geq 0$ (left); reflux ratio along the pinch branches (right).

Refer to Figure 4 for a legend on the pinch points, bifurcation points, and the eigenvectors.

for which the branching point appears can be directly calculated by adding

$$\nabla_{\mathbf{r}}\mathbf{f}(\mathbf{u}, \varphi, r, E)^T\mathbf{w} = \mathbf{0} \tag{17}$$

to Eqs. 14–16.

Now, a lower bound of the entrainer feed flow rate $(E/F)_{min,bif}$ for feasible operation is known. This lower bound corresponds to a local minimum of E/F on the saddle-node bifurcation path with respect to r. In the PWG example this minimum is found in the ternary region of the composition space. Note, however, that for other examples the saddle-node bifurcation path may reach an edge of the composition space without displaying a minimum. On that edge the saddle-node line itself will branch with another saddle-node line that runs on the same edge. (The PWG example also shows this behavior. The saddle-node bifurcation line branches on the isopropanol–glycol edge and an additional line of saddle-node bifurcations/branching points is obtained on that edge. In Figures 5–8 the branching points on this additional saddle-node bifurcation line are shown, although the line itself has been omitted for better legibility. The additional saddle-node bifurcation line does not contribute to the determination of $(E/F)_{min,bif}$ because a ternary branching point is already found before reaching the

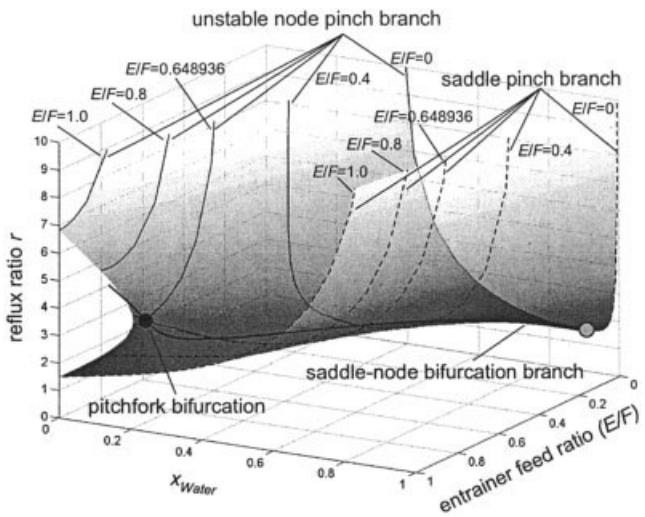

Figure 9. Finding a codimension-2 pitchfork bifurcation by continuation in both parameters r and (E/F).

The lines on the surface correspond to cuts of constant E/F.

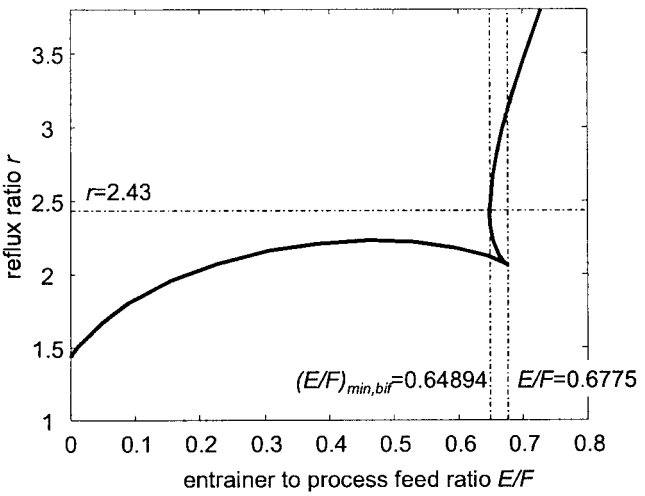

Figure 10. Locus of saddle-node bifurcations in r–(E/F) parameter space.

binary edge.) The separation of acetone and methanol with water (see Appendix A) shows this behavior. In such a case the search for a minimum must be continued on that new branch.

Although a ternary example has been used above to illustrate the determination of $(E/F)_{min,bif}$, the procedure described above is not limited by the number of components. The general applicability for arbitrary multicomponent mixtures will be highlighted with a quaternary example. Note, however, that for mixtures displaying multiple minimum boiling azeotropes each of these azeotropes is a valid starting point for a saddle-node bifurcation path.

In principle, the pitchfork bifurcation point can be directly obtained by simultaneously solving Eqs. 14–17. However, application of standard nonlinear equation solvers based on the Newton–Raphson method will usually fail unless good initial values for the state variables **u**, the bifurcation parameters r and E, and the null vector **w** are known. Such initial values can be obtained by applying a suitable continuation strategy. Based on the observations presented above the following procedure for the determination of a lower bound for the entrainer feed flow rate $(E/F)_{min,bif}$ (procedure 1) is suggested:

(1) Starting from each minimum boiling azeotrope calculate the respective pinch branch.

(2) Determine all saddle-node bifurcations on these pinch branches.

(3) Starting from each saddle-node bifurcation calculate the respective saddle-node bifurcation branch until a branching point (pitchfork bifurcation) is detected. If the saddle-node bifurcation branch itself branches before such a point is found follow all branches in the direction of decreasing entrainer feed flow rates.

(4) Using the initial values for **u**, r, E, and **w** obtained in step 3 solve Eqs. 14–17 with a Newton–Raphson-type solver.

(5) The entrainer to process feed ratio E/F at the pitchfork bifurcation marks a topological lower bound for feasible operation. It will be called $(E/F)_{min,bif}$.

Determination of a lower and an upper bound for the reflux ratio

For a fixed entrainer-to-feed flow rate ratio $E/F > (E/F)_{min,bif}$ the pinch map of the extractive section displays a feasible topology (see Figure 7). Thus, a range of reflux ratios complying with the criterion for feasible topology of Knapp and Doherty (1994) can be found from the pinch map. First, a ternary unstable node on the azeotrope pinch branch must not occur. The reflux ratio on this pinch branch ranges from $r \rightarrow \infty$ at the azeotrope to $r = 3.08$ at the branching point. Therefore, $r_{max,bif} = 3.08$ is an upper bound for the reflux ratio. Additionally, a ternary saddle pinch is required for a feasible topology. Such a pinch point may occur on a pinch branch originating at any of the intermediate boilers. Note that in this example both water and isopropanol are intermediate boilers because the minimum-boiling azeotrope is treated as a pseudocomponent. Following these pinch branches from the pure components it can be observed that a ternary saddle pinch is obtained for any reflux between $r \rightarrow \infty$ at the water vertex and $r = 2.06$ at the ternary saddle-node bifurcation on the water pinch branch. Therefore $r_{min,bif} = 2.06$ represents a lower bound for the reflux ratio. For the general case of an arbitrary multicomponent mixture the following procedure for the determination of $r_{min,bif}$ and $r_{max,bif}$ for a specified entrainer feed flow rate E (procedure 2) is suggested:

(1) Calculate all pinch branches and mark those that originate at a minimum boiling azeotrope.

(2) Calculate all saddle-node bifurcations. Consider that branching points are also saddle-node bifurcations.

(3) From the list of saddle-node bifurcations on pinch branches originating at a minimum boiling azeotrope select the one with the lowest reflux ratio to obtain $r_{max,bif}$.

(4) From the list of saddle-node bifurcations on pinch branches that do not originate at a minimum boiling azeotrope select the one with the highest reflux ratio to obtain $r_{min,bif}$.

Selection of Feasible Entrainer Flow Rates and Reflux Ratios

A feasible separation requires that distillate and bottom product are connected by a continuous concentration profile representing the compositions on each tray of the column. The criteria for obtaining a lower and an upper bound for the reflux ratio and a lower bound for the entrainer feed flow rate that were deduced from topological analysis of pinch maps provide a range of operating conditions for which such a feasible column profile might be obtained. However, they do not guarantee that the separation is feasible for all specifications within those bounds. It will be shown that especially the reflux ratio usually must be chosen higher than its topological lower bound. Therefore, topological feasibility is only a necessary and not a sufficient condition for the design of a feasible extractive distillation column.

Methods for assessing the feasibility of the separation

Levy and Doherty (1986) discuss design methods for obtaining the minimum reflux for feasible operation of multiple-feed distillation columns. A straightforward method is to iteratively solve the mass and energy balance equations from plate to plate. Starting this calculation from the distillate and bottoms product, respectively, the profiles of the rectifying and the stripping section are determined. For a feasible column, these profiles must be connected by the profile of the extractive middle section. This profile can be calculated analogously, although the designer must provide the feed tray number of either the lower or upper feed to have a starting point for the tray-by-tray iteration of the extractive section. A rather strong sensitivity of the course of the profiles with respect to this choice is observed, which makes the determination of the minimum reflux by tray-by-tray design a relatively tedious task. An additional drawback of this method is a strong sensitivity of the profiles with respect to trace components in the distillate and bottoms section (for a more complete discussion, see Bausa et al., 1998). To overcome these limitations, Levy and Doherty (1986) present an algebraic criterion for the determination of minimum reflux of ternary separations in two-feed columns. It is based on the argument that at minimum reflux one of the feed concentrations and specific pinch points of two column sections must lie on a straight line. This method works reliably and generates quite accurate results. However, for the application of this method the type of split (direct/indirect), the controlling feed, and in the case of multiple pinch solutions for one section also the controlling pinch, must be

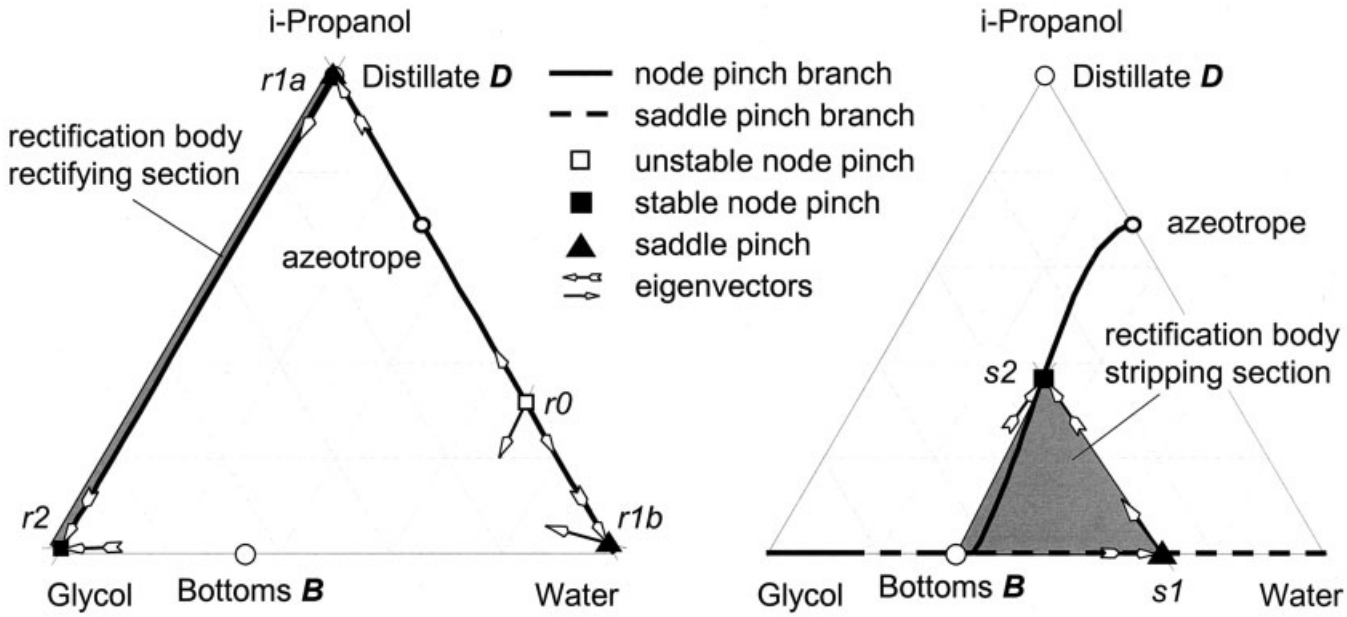

Figure 11. Pinch branches, pinch points, and rectification bodies for rectifying (left) and stripping section (right) at $E/F = 0.750$ and $r = 2.042$.

known a priori. Furthermore, the method is restricted to ternary mixtures.

Bausa et al. (1998) present a new criterion for the determination of the minimum reflux ratio (minimum energy demand) of single-feed columns that is applicable to arbitrary splits and mixtures with an arbitrary number of components. The method is based on the approximation of all column profiles by so-called rectification bodies, which are constructed from the pinch points of each section. It may be interpreted as an extension of the method of Underwood (1948) and its graphical interpretation by Franklin and Forsyth (1953). However, it is not limited to ideal mixtures. Using some insight from the nonlinear analysis of the extractive distillation pinch equations the rectification body method can be extended to columns with two feeds and therefore applied to extractive distillation.

Construction of the rectification bodies and assessment of split feasibility

For the rectifying and stripping sections, the construction of the rectification bodies can be performed as presented in the original algorithm (see Bausa et al., 1998). First, the pinch branches of the respective section are determined for a fixed choice of a feasible entrainer feed flow rate E. Given some reflux ratio r for which the feasibility of the split is to be tested, all pinch points on these pinch branches and their stability are calculated. Unstable node pinches are discarded. Now all possible paths of the profiles are determined. Some rules for the course of plate-to-plate profiles are exploited. The first rather trivial rule is that all profiles start at the respective product composition. Secondly, under minimum reflux the profiles will touch one or more pinch points. The number of stable eigenvectors in the pinch points touched by a profile must increase strictly monotonically. Figure 11 (left) shows the pinch branches and pinch points of the rectifying section for the PWG separation at an entrainer-to-process feed ratio of $E/F = 0.750$ and a reflux ratio of $r = 2.042$. Four pinch points are found: one unstable node *r0*, two saddle pinches *r1a* and *r1b*, and one stable node *r2*. According to the rules for constructing rectification bodies, *r0* is discarded. Furthermore, *r1a* can also be excluded because it has the same concentration as the distillate product composition, which automatically is the starting point of all paths. Two potential paths, *D–r2* and *D–r1b–r2*, remain. The second path *D–r1b–r2* gives rise to a rectification body that nearly spans the complete composition space. The corresponding profile touches the unstable node pinch *r0* and therefore this path is obviously infeasible. To properly discard such infeasible path an additional pinch reachability check is incorporated into the method.

A pinch branch is identical to the column profile of a reversible separation (see Köhler et al., 1991; Thong et al., 2000). The profile of such a column will end at the first pinch point it encounters on the pinch branch regardless of its stability because the driving force at the pinch is vanishing. Therefore additional pinch points on the same pinch branch cannot be reached. This argumentation can be generalized to arbitrary column profiles. As soon as a profile approaches a pinch point, it will either stop if the pinch is a stable node or be deflected from the pinch branch if the pinch is a saddle. In either case, additional pinch points on the same branch will never be reached. Thus an additional rule for the construction of rectification bodies is formulated: *If a pinch branch has a connection to the product composition, use only the first pinch point from the product composition on that pinch branch for the construction of a separation path. Discard all other pinch points on that branch.* Note that several pinch branches may be connected to the pinch branch passing through the product composition by branching points. Using this additional rule, the saddle pinch *r1b* is discarded and only path *D–r2* remains. The corresponding rectification body in the rectifying section is

shown in Figure 11 (left): it is a straight line on the binary isopropanol–glycol edge.

The construction of the rectification bodies for the stripping section is more straightforward. Two pinch solutions, one saddle pinch *s1* and one stable node *s2*, are found. They correspond to one path *B–s1–s2* and the corresponding triangular rectification body is shown in Figure 11 (right).

The rectification bodies of the extractive middle section cannot be constructed using the same approach as for the rectifying and stripping sections. The overall product composition $\mathbf{x}_N$ of the middle section as determined from Eqs. 7 and 8 often lies outside the physically attainable composition space. Hence, some of the pinch branches and pinch points also move outside the composition space. Therefore, the pinch map of the extractive section is not always complete. As deduced from the nonlinear analysis of an extractive distillation column, a saddle pinch must always be present for a feasible ternary separation. For multicomponent separations, there may be more than one saddle pinch, as will be shown in a quaternary example. Levy and Doherty (1986) observe that the eigenvectors of such extractive section saddle pinch points give a very good approximation of the directions in which the profiles approach and leave the saddle pinch. This observation is also supported by examination of the column profile of the PWC separation in Figure 4b. The profile matches the eigenvectors of the saddle nearly exactly and shows only small curvature. Therefore, the course of the middle section profile can be approximated by rectification bodies that are obtained as follows (procedure 3):

(1) Calculate all saddle pinch points.

(2) Determine all paths connecting the saddle pinch points using the rule that the number of stable eigenvectors on a path must increase strictly monotonically.

(3) Approximate the starting point of the column profile by following the most stable (smallest eigenvalue) eigenvector of the first saddle of the path until some edge of the composition space is reached.

(4) Approximate the end point of the profile by following the most unstable (largest eigenvalue) eigenvector of the last saddle of the path until some edge of the composition space is reached.

(5) Consider both extensions from the saddle toward the edges of the composition space along each eigenvector in steps (3) and (4). For ternary separations, where there are two linearly independent eigenvectors, one path therefore typically corresponds to four middle section rectification bodies.

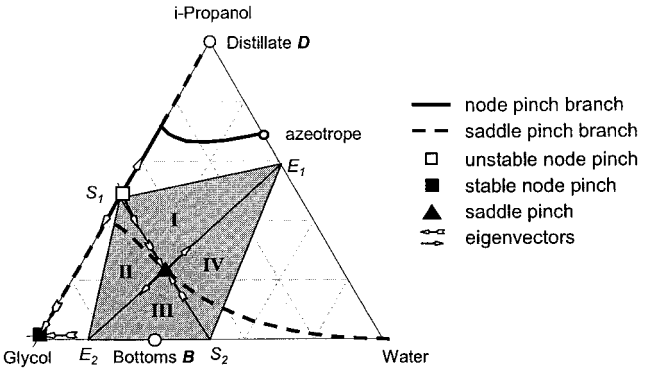

Figure 12. Pinch branches, pinch points, and rectification bodies for the extractive section at *E/F* = 0.750 and *r* = 2.042.

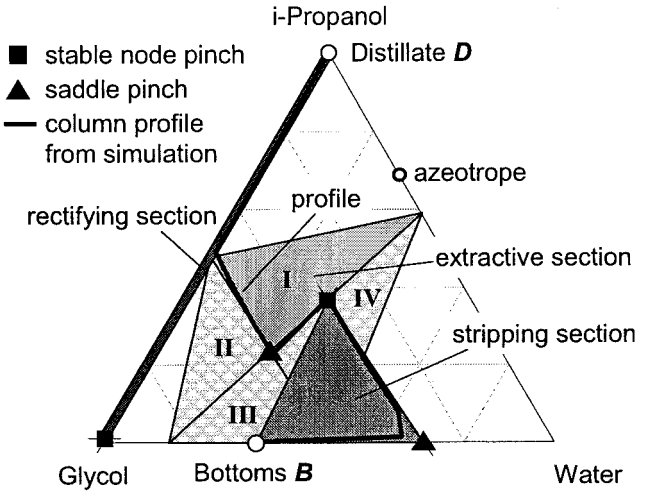

Figure 13. Rectification bodies at *E/F* = 0.750 and minimum reflux *r* = 2.042 and column profile simulated with Aspen+.

Figure 12 shows the application of these rules to the middle section of the PWG separation at $E/F = 0.750$ and $r = 2.042$. Only one ternary saddle pinch and therefore only one path is obtained. The extension of the stable eigenvector of this saddle pinch toward the edges of the composition space results in two potential starting points S_1 and S_2 for the column profile of the extractive section. Similarly, two potential end points E_1 and E_2 of the profile are found by extending the unstable eigenvector of the pinch. Therefore, four rectification bodies are obtained as a whole.

The rectification bodies for all three sections of the column are shown in Figure 13. It can be seen that both the rectifying and middle and the middle and stripping sections intersect each other. In the middle section rectification body (I) is controlling because it is the only one that intersects with both the rectifying and stripping section bodies. Since the rectification bodies are an approximation of column profiles there must therefore exist one profile that continuously connects the distillate with the bottom product. This claim is supported by the column profile obtained from an Aspen+ simulation at r_{min} with the same specifications (see Table 1) that is also shown in the figure. For the simulation a column with 80 trays was used. The process feed is introduced on stage 38, whereas the entrainer feed is added on stage 10.

Determination of the maximum and minimum reflux ratios for a fixed entrainer flow rate

Regarding the topological considerations from above, the range of candidate reflux ratios for feasible operation is constrained by $r_{min,bif} \leq r \leq r_{max,bif}$. Within these bounds, the topology of the extractive section pinch map does not change and the extractive column behaves similarly to a regular single-feed column. Hence, increasing the reflux ratio corresponds to a sharper separation. The maximum separative effect is attained at $r = r_{max,bif}$. Therefore the maximum reflux ratio is given by $r_{max} = r_{max,bif}$. For the PWG separation with an

Table 1. Specifications and Results for the Example Separations*

Figure	Component	$\mathbf{x}_F$	$\mathbf{x}_E$	$\mathbf{x}_D$	D/F $(E/F)_{min,bif}$	$(E/F)_{min}$ r_{min} r_{max}	E/F r_{min} r_{max}	CPU (s)
13, 16	Isopropanol	**0.62**	**0.0**	**1.0**	**0.62**	0.649	0.750	2.67
	Water	**0.38**	**0.0**	**0.0**	0.649	2.428	2.042	
	Ethylene glycol	**0.0**	**1.0**	**0.0**		2.428	4.084	
17	Ethanol	**0.124**	**0.0**	**0.2**	**0.62**	0.662	0.756	5.26
	Isopropanol	**0.496**	**0.0**	**0.8**	0.662	2.289	1.972	
	Water	**0.38**	**0.0**	**0.0**		2.289	3.943	
	Ethylene glycol	**0.0**	**1.0**	**0.0**				
19	Acetone	**0.7774**	**0.0**	**1.0**	**0.7774**	0.740	0.814	0.77
	Methanol	**0.2226**	**0.0**	**0.0**	0.740	2.600	1.991	
	Water	**0.0**	**1.0**	**0.0**		2.618	4.707	
19	Acetone	**0.7774**	**0.0**	**1.0**	**0.7774**	0.586	0.721	3.28
	Methanol	**0.2226**	**0.0**	**0.0**	0.721	4.344	3.947	
	Ethanol	**0.0**	**1.0**	**0.0**		4.346	7.892	
19	Acetone	**0.7774**	**0.0**	**1.0**	**0.7774**	2.187	2.742	4.48
	Methanol	**0.2226**	**0.0**	**0.0**	2.187	6.073	5.407	
	Isopropanol	**0.0**	**1.0**	**0.0**		6.114	10.814	
19	Acetone	**0.7774**	**0.0**	**0.0**	**0.2226**	1.173	1.615	6.09
	Methanol	**0.2226**	**0.0**	**1.0**	0.788	7.645	5.665	
	Chlorobenzene	**0.0**	**1.0**	**0.0**		7.645	11.329	

*Specifications are marked in bold. For all examples, a pressure of $p = 1.013$ bar, saturated liquid feed and product streams, a total condenser, and operational constraints of $\beta_{E,min} = 1.1$ and $\beta_{r,min} = 2.0$ are specified. The PWG and EPWG examples are modeled using the Wilson activity model. All other examples are modeled using the UNIQUAC activity model. Physical property parameters were obtained from Aspen+. CPU time was determined on a P-III 900-MHz PC.

entrainer feed ratio of $E/F = 0.750$ a maximum reflux ratio of $r_{max} = 4.084$ is found.

Similar to simple columns there exists a minimum reflux ratio for the extractive column that must be exceeded to match the specified product purities. In terms of column design, where the desired product purity is prespecified, an insufficiently low choice for the value of r is characterized by the nonexistence of a continuous concentration profile connecting the distillate and bottom products. In terms of the rectification body method this corresponds to the absence of intersection between the bodies. Hence, if the bodies do not touch, the separation is infeasible and below minimum reflux (Figure 14, left). If they penetrate each other the separation is feasible but above minimum reflux (Figure 14, right). To find the minimum reflux the smallest reflux ratio that makes intersection of the bodies possible must be found. Starting with one reflux that is known to be below minimum reflux (that is, $r_{min,bif}$), and another one that is known to be above minimum reflux (that is, $r_{max,bif}$), the minimum reflux that makes the rectification bodies just touch can be determined using a bisection algorithm. The minimum reflux situation for the PWG example at $E/F = 0.750$ and $r_{min} = 2.042$ is shown in Figure 13.

Determination of the minimum entrainer flow rate

As stated above, the maximum separative effect is attained at $r = r_{max,bif}$. For any choice of the entrainer feed flow rate $E \geq E_{min,bif}$ above its topological minimum, a feasible choice for the reflux ratio r will therefore exist only if the separation is feasible at $r = r_{max,bif}$ (that is, if the respective rectification bodies intersect at this reflux ratio). The evaluation of the rectification bodies at $r_{max,bif}$ can therefore be used as a fast criterion for the determination of the feasibility of the choice for the entrainer feed flow rate E. Once a feasible choice E_{feas} is found, the minimum entrainer feed flow rate E_{min} with $E_{min,bif} \leq E_{min} \leq E_{feas}$ can be determined using a bisection algorithm.

For most separations that we have investigated the minimum entrainer feed flow rate E_{min} is very close to the lower bound $E_{min,bif}$ obtained from the bifurcation analysis. The separation of isopropanol and water using ethylene glycol as an entrainer falls into this category. The minimum entrainer feed ratio is $(E/F)_{min} = 0.64894$ and therefore identical to $(E/F)_{min,bif}$ with respect to the amount of significant digits chosen here. Figure 15 shows the rectification bodies at the minimum entrainer flow $(E/F)_{min} = 0.64894$ and the maximum reflux ratio $r_{max,bif} = 2.428$. Note, however, that there are some mixtures that show different behavior. For example, the separation of acetone and water using chlorobenzene as the heavy entrainer, which will be discussed in more detail in Appendix B, exhibits a minimum entrainer feed ratio of $(E/F)_{min} = 1.173$, well above its topological bound of $(E/F)_{min,bif} = 0.7876$.

Operational Constraints

Operational stability of separation processes is a crucial factor to the economical success of such processes. This is especially true to extractive distillation because extractive distillation columns often show counterintuitive operational properties (Laroche et al., 1992). Because of the extractive effect and the existence of a maximum reflux ratio the separation is not necessarily improved by increasing the reflux ratio, which is a common property of simple distillation. Furthermore, the range of feasible reflux ratios may be small. In this case elaborate control mechanisms are required. Therefore, it is sometimes useful to sacrifice cost-optimality of a steady-state design in favor of better operational stability.

Andersen et al. (1995) and Knight and Doherty (1989)

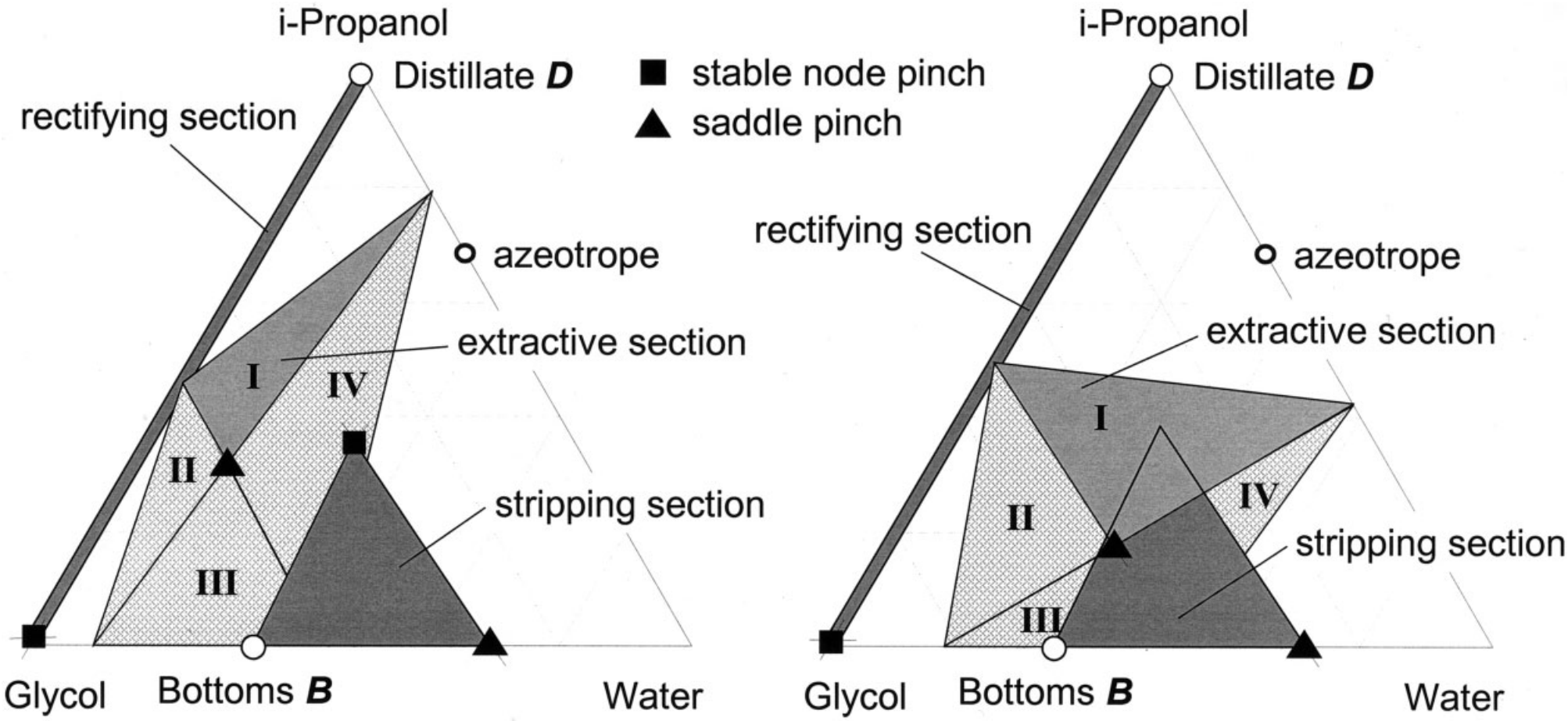

Figure 14. Rectification bodies at $r = 1.9$ below minimum reflux (left) and at $r = 2.2$ above minimum reflux (right).
The entrainer to process feed ratio is $E/F = 0.750$ in both cases.

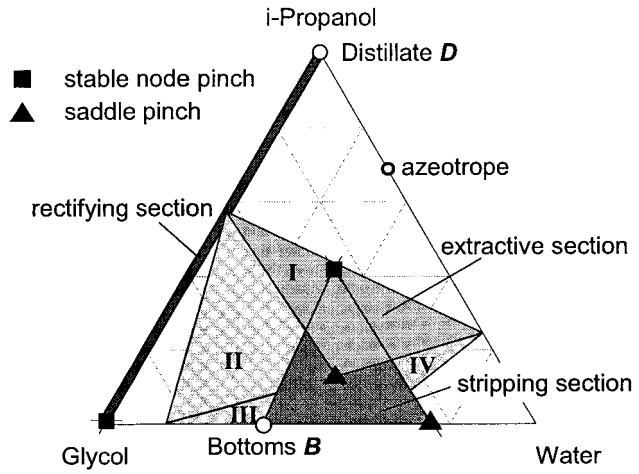

Figure 15. Rectification bodies at $(E/F)_{min} = 0.64894$ and $r_{max,bif} = 2.428$.

discuss the impact of operational properties on the design of extractive columns. To illustrate the trade-off between cost-optimality and operability they make extensive use of diagrams in which the energy requirement of the column (internal vapor flow in Andersen et al., 1995; energy cost in Knight and Doherty, 1989) is plotted against the entrainer feed flow rate. Using the knowledge from the preceding sections such a diagram can also be produced for the PWG example and is shown in Figure 16. It can be seen that the feasible region is contained by the minimum and maximum reflux ratios as a function of the entrainer flow rate. The lower bound for the entrainer flow rate that was found from bifurcation analysis is also shown. As already discussed, it is identical to the minimum feasible entrainer flow rate for this example. The lower bound for the reflux ratio as obtained from the nonlinear analysis of the pinch map is also shown in the figure. Note that the minimum reflux ratio r_{min} is identical to the lower bound $r_{min,bif}$ from the topological analysis for a small range of the entrainer feed ratio $(E/F)_{min} \leq E/F \leq 0.6775$. As can be seen from Figure 7, the lower bound $r_{min,bif}$ is governed by a ternary saddle-node bifurcation on the pinch branch originating from the pure water vertex. Note that the reflux ratio $r = 2.06$ corresponding to this ternary saddle-node bifurcation is much larger than the reflux ratio $r = 1.84$ corresponding to the saddle-node bifurcation at the intersection of the pinch branch with the binary isopropanol–glycol edge. The ternary saddle-node bifurcation is represented by the lower branch of the saddle-node–bifurcation curve in Figure 10. At $E/F = 0.6775$ this ternary saddle-node bifurcation vanishes. The topological lower bound $r_{min,bif}$ is then determined by the intersection of the pinch branch originating at the pure water vertex with the binary isopropanol/glycol edge, resulting in smaller values for $r_{min,bif}$ for which the

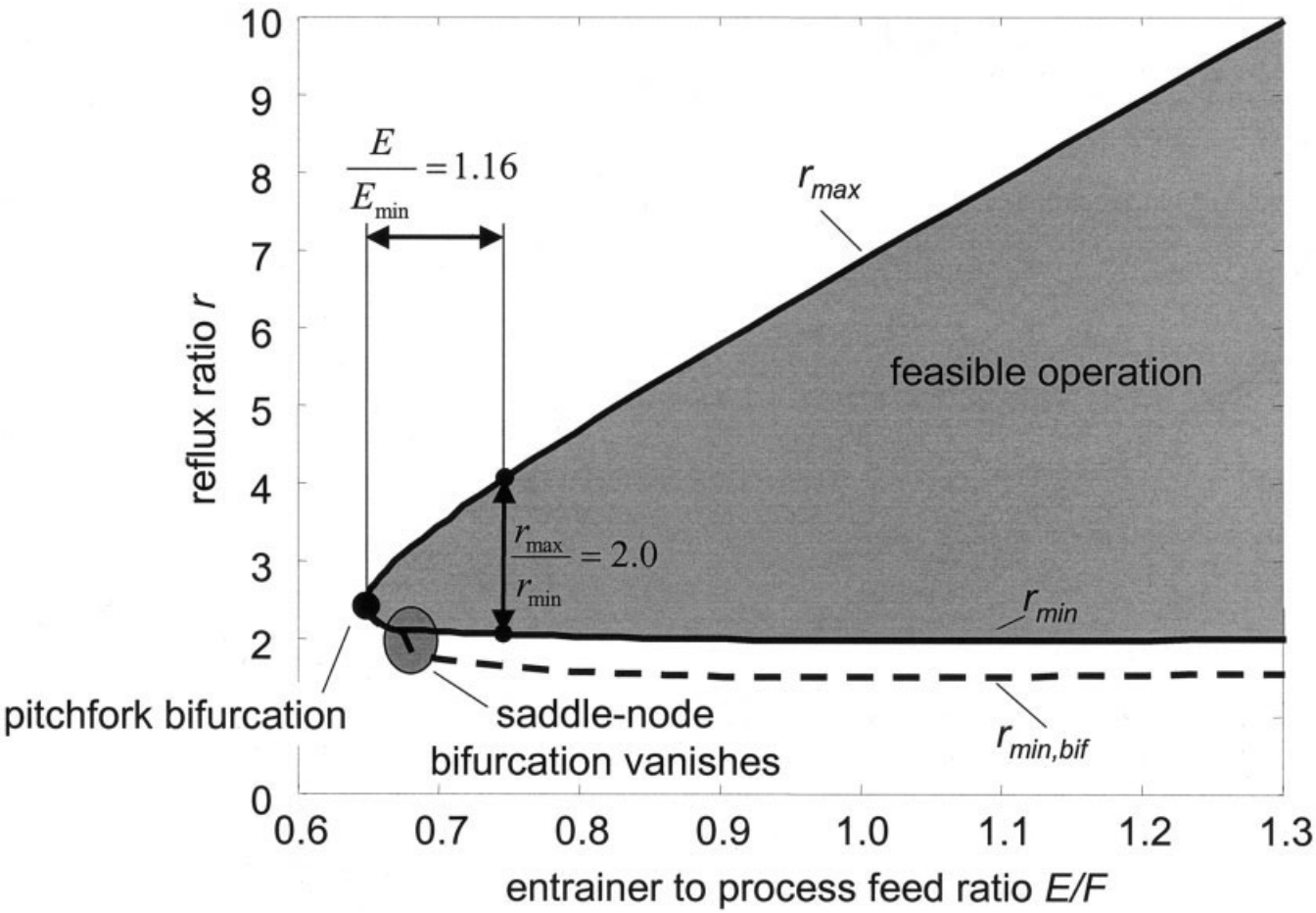

Figure 16. Minimum and maximum reflux ratios for the PWG separation as a function of the entrainer feed flow rate.

rectification bodies do not intersect. Therefore, the $r_{min,bif}$ curve detaches from the r_{min} curve.

The operating cost of the extractive column are essentially specified by the reflux ratio which determines the condenser and reboiler heat duties. In addition to the extractive column an entrainer recovery column is necessary in which the bottom product of the extractive column is further separated into water and the entrainer ethylene glycol. This column is a conventional binary column and its energy demand can readily be analyzed with the conventional rectification body method for simple columns (Bausa et al., 1998). The operating cost of the solvent recovery column increases with the entrainer feed flow rate to the extractive column because consequently more material must be purified downstream. Therefore, a cost-optimal extractive distillation process is operated at low entrainer feed flow rate and low reflux of the extractive column. This corresponds to operation of the extractive column close to the tip of the nose of the trade-off diagram in Figure 16. However, operating the extractive column at these conditions will be difficult, given that the range of feasible refluxes is quite small. Furthermore, the number of trays required to achieve the desired purities will be large because for operation close to the minimum or maximum reflux ratios the separation can be achieved only in a column with an infinite number of trays, whereas operation at intermediate refluxes will require fewer trays.

These operational implications for design indicate that a good design of the extractive column will be operated at some distance from the feasibility boundaries. This can be ensured by restricting the design variables entrainer feed flow rate and reflux ratio with operational constraints. Some useful formulations of such constraints on the entrainer feed flow rate may be $\alpha_E = E_{op} - E_{min} > \alpha_{E,min}$ or $\beta_E = E_{op}/E_{min} > \beta_{E,min}$ where E_{op} is the entrainer feed flow rate at operating conditions and E_{min} is the minimum entrainer feed flow rate. Useful formulations for constraints for the reflux ratio may be $\alpha_r = r_{max} - r_{min} > \alpha_{r,min}$ or $\beta_r = r_{max}/r_{min} > \beta_{r,min}$ where r_{max} and r_{min} are the maximum and minimum reflux ratios for feasible separation, respectively. In some cases it may also be useful to restrict the entrainer feed flow rate and the reflux directly with lower and upper bounds. Unfortunately there are no standard heuristics for choosing these operational constraints. For the PWG example the operational constraints have been chosen as $\beta_{E,min} = 1.1$ and $\beta_{r,min} = 2.0$. The resulting operating conditions, $E/F = 0.750$ and $r = 2.042$ are indicated in Figure 16. The constraint on the reflux ratio is the driving design constraint. The results for the PWG example problem are summarized in Table 1.

A New Algorithm for the Determination of Optimum Entrainer Flow Rate and Reflux Ratio

Using the insights gained from the nonlinear analysis of an extractive column, the extension of the rectification body method to two-feed columns and by incorporating operational considerations a novel procedure for the design of extractive distillation columns can be formulated as follows (procedure 4):

(1) Specify composition, flow rate, and thermal state of the process feed as well as composition and thermal state of the entrainer feed. Also specify all operational constraints on entrainer-to-process feed ratio E/F and reflux ratio r.

(2) Specify which mixture or pure component will be recovered in the distillate product. Confirm this specification with an analysis of the isovolatility curve.

(3) Determine composition, flow rate, and thermal state of the distillate product.

(4) Determine the lower bound for the entrainer to process feed ratio $(E/F)_{min,bif}$ from nonlinear analysis of the extractive section pinch map using procedure 1.

(5) Set $E/F = (E/F)_{min,lo} = (E/F)_{min,bif}$.

(6) Determine the lower bound $r_{min,bif}$ and the upper bound $r_{max,bif}$ from nonlinear analysis of the extractive section pinch map (procedure 2).

(7) Set $r = r_{max,bif}$.

(8) Check split feasibility by applying the rectification body method using the following steps:

(8.1) Determine all pinch branches and pinch points for each column section.

(8.2) For the rectifying and stripping sections, construct the rectification bodies using the standard procedure.

(8.3) For the extractive middle section, construct the rectification bodies using the eigenvectors of the saddle pinch points (procedure 3).

(8.4) Check all members of the sets of rectification bodies for intersection against each other. If there exists a middle section body that intersects both a distillate section body and a stripping section body, the specified separation is feasible.

(9) If the separation is feasible then an upper bound for the minimum entrainer to process feed ratio $(E/F)_{min,up} = E/F$ is found; otherwise, increase E/F and repeat from 6.

(10) Use bisection to determine $(E/F)_{min}$ between $(E/F)_{min,lo}$ and $(E/F)_{min,up}$, incorporating steps 6–8 for checking the feasibility of the separation.

(11) Set $E/F = (E/F)_{min}$. This value also marks a lower bound for the operational entrainer to process feed ratio $(E/F)_{op,lo}$.

(12) Determine the lower bound $r_{min,bif}$ and the upper bound $r_{max} = r_{max,bif}$ from nonlinear analysis of the extractive section pinch map.

(13) Determine the minimum reflux ratio r_{min} between $r_{min,bif}$ and $r_{max,bif}$ using bisection incorporating the rectification body method (steps 8.1–8.4) for checking the feasibility of the separation.

(14) Check if operational constraints are met. If not, choose a larger entrainer to process feed ratio E/F and repeat from step 12; otherwise, an upper bound for the operational entrainer to process feed ratio $(E/F)_{op,up}$ is found.

(15) Use bisection to determine $(E/F)_{op}$ between $(E/F)_{op,lo}$ and $(E/F)_{op,up}$ using the following steps:

(15.1) Choose E/F between $(E/F)_{op,lo}$ and $(E/F)_{op,up}$.

(15.2) Determine the minimum reflux ratio r_{min} and the maximum reflux ratio r_{max} using steps 12 and 13.

(15.3) Check if operational constraints are met. If not, set $(E/F)_{op,lo} = E/F$; otherwise, set $(E/F)_{op,up} = E/F$.

(15.4) If $(E/F)_{op,up} - (E/F)_{op,lo}$ is larger than the required accuracy repeat from 15.1. Otherwise the operating entrainer to process feed ratio $(E/F)_{op}$ is found.

Using this design procedure, the optimum operating entrainer feed flow rate as well as the corresponding minimum and maximum reflux ratios are directly determined. The results are identical to the graphical analysis of the trade-off curve

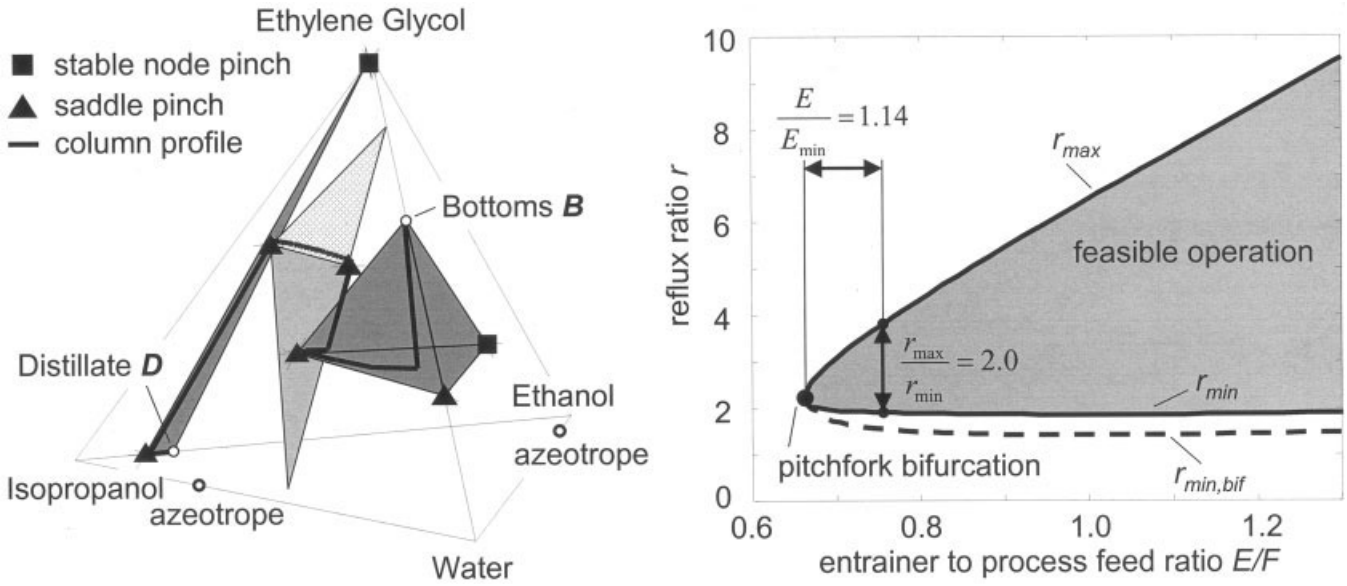

Figure 17. Pinch points, rectification bodies, and column profile at $E/F = 0.757$ and $r_{min} = 1.972$ (left-hand side) and feasible operating region (right-hand side) for the EPWG mixture.

presented in Figure 16. The minimum feasible entrainer feed flow rate and the corresponding reflux ratio are also determined. This design procedure has been implemented in C. Results for the PWG example and the computational performance of this code can be inferred from Table 1. Results are generally obtained well below 10 s of computation time. Therefore, the design procedure can be used interactively.

Examples

In this section the new design method will be applied to different separation examples. The performance of the analysis of multicomponent mixtures will be highlighted with a quaternary example. A brief case study of extractive distillation process alternatives for a binary process feed will show how the design procedure can be used to compare the performance of different entrainers. The specifications and results for all examples are summarized in Table 1.

A quaternary example

A second alcohol, ethanol, is added to the isopropanol–water mixture that has already been discussed at length. As can already be inferred from the molecular similarity of ethanol and isopropanol, ethanol can also be separated from water by extractive distillation with ethylene glycol as heavy entrainer. A possible straightforward approach to separation process design for the ternary mixture ethanol–isopropanol–water is to first split this mixture into the binary mixtures ethanol–water and isopropanol–water and then feed these mixtures to separate extractive distillation trains. This process alternative, however, does not really seem appealing from an economic point of view because it needs five columns: preseparation into two binary mixtures, two extractive columns, and two entrainer recovery columns. Investigation of the preseparation column using RBM for simple columns further reveals that this is a very energy-intensive separation requiring a minimum energy demand of $Q_B/F = 360$ MJ/kmol.

When separating an ethanol–water mixture by extractive distillation, ethanol is recovered at the top of the extractive column. This setup is similar to the isopropanol–water case. Therefore it seems worthwhile to try the separation of both alcohols from water in one extractive column where the quaternary mixture of ethanol, isopropanol, water, and glycol (EPWG) is present. The operational constraints, $\beta_{E,min} = 1.1$ and $\beta_{r,min} = 2.0$, were chosen identical to the PWG separation. Using these specifications, the design procedure is applied as presented above. The algorithm rates this split feasible and suggests an operating entrainer to process feed ratio of $(E/F)_{op} = 0.757$. This is only marginally more than for the PWG example. Minimum and maximum reflux ratios are $r_{min} = 1.972$ and $r_{max} = 3.943$, which is even less than for the PWG example. Figure 17 (left) shows the active pinches and rectification bodies at $(E/F)_{op}$ and r_{min}. It can be seen that, because of the additional component ethanol, the number of pinch points and the dimensionality of the rectification bodies has increased. In the rectifying section one saddle pinch and one stable node pinch are found and form a triangular rectification body. In the stripping section two saddle pinches and one stable node pinch are found. This corresponds to a tetrahedronal rectification body. The extractive section is characterized by the occurrence of two saddle pinch points. The saddle exhibiting two unstable eigendirections and one stable eigendirection lies on the ternary ethanol–isopropanol–glycol edge and is contained within the rectification body of the rectifying section. Therefore, this saddle pinch point marks the starting point of the extractive section profile. The two potential end points of the profiles are constructed using the unstable eigenvector of the other saddle pinch. Two triangular rectification bodies are formed. The results of the design method were confirmed with an Aspen+ simulation at r_{min} for the same specifications (see Table 1). To generate results that are comparable with the rectification bodies, a column with a large number of trays (200 trays, process feed on stage 150, entrainer feed on stage 50) was chosen. The column profile obtained from this simulation

is also shown. It can be seen that the course of this profile is nearly identical to the path predicted by the rectification bodies.

Figure 17 (right) shows the feasible operating region as a function of entrainer-to-process feed ratio and reflux ratio. It is nearly identical to the one obtained for the ternary PWG example (cf. Figure 16). For $(E/F)_{op}$, the minimum energy demand of the extractive column is $Q_B/F = 63$ MJ/kmol. Using RBM for simple columns, the minimum energy demands of the solvent recovery column and the ethanol–isopropanol separation are determined as Q_B/F values of 23 and 152 MJ/kmol, respectively. This corresponds to an overall minimum energy demand of $Q_B/F = 238$ MJ/kmol of the complete process. Compared to the preseparation process this is less than the amount of energy that is needed for the preseparation step alone. Therefore, there is a strong indication that it is economically advantageous to separate both alcohols and the water in one quaternary extractive column.

Comparing entrainers

The binary mixture acetone–methanol can also be separated in an extractive distillation process. To be able to give a rough comparison of the performance of different entrainers, the complete flowsheet of the separation process consisting of the extractive column and the entrainer recovery column will be analyzed (see Figure 18). The process feed has nearly azeotropic composition. Laroche et al. (1991) identify water, chlorobenzene, ethanol, and isopropanol as candidate entrainers for extractive distillation. Chlorobenzene is a known carcinogen and therefore does not seem to be an attractive entrainer candidate nowadays. For the application of the design method, however, this fact is not important. To generate results that can be easily compared to those of the original article of Laroche et al. (1991), we will consider chlorobenzene a valid choice for the heavy entrainer.

Analysis of the isovolatility curves of the four ternary mixtures reveals that the acetone–methanol mixture is influenced differently depending on the entrainer. Water, ethanol, and isopropanol preferably bind to methanol and therefore high-purity acetone is obtained in the distillate product. When chlorobenzene is used, methanol is obtained at the top, although it has a higher boiling point than that of acetone. The distillate products for the four design cases are defined with respect to this behavior (cf. Table 1). To obtain a fair comparison, identical operational constraints, $\beta_{E,min} = 1.1$ and $\beta_{r,min} = 2.0$ are used for all calculations.

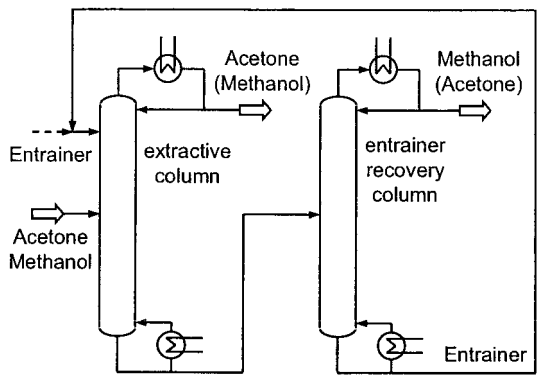

Figure 18. Flowsheet for the separation of an acetone–methanol mixture by extractive distillation.

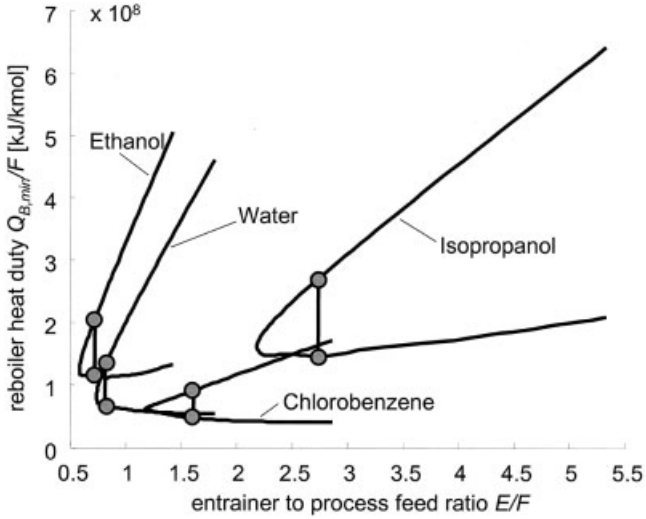

Figure 19. Minimum and maximum reboiler heat duty of the extractive column as a function of entrainer to process feed ratio.

Vertical lines indicate the operating entrainer to process feed ratio.

The design of the extractive distillation process can be separated into two steps. In the first step the extractive column is designed using the new design procedure. Some interesting features of the acetone–methanol–water (AMW) and the acetone–methanol–chlorobenzene (AMC) separations are discussed in the Appendix.

The minimum reflux of the extractive column is used to approximate the operating cost of this column. Note, however, that the distillate product flow rate differs depending on the choice of entrainer because of the different distillate compositions (cf. Table 1). Therefore, a direct comparison of reflux ratios is not really suited for comparison of the different processes. Instead, the rating of the designs will be based on the energy requirement of the column [for a more detailed discussion, see Laroche et al. (1991)]. Figure 19 shows the minimum and maximum reboiler heat duties as a function of the entrainer-to-process feed ratio for all four entrainer candidates. It can be seen that the chlorobenzene process displays the lowest energy demand followed by the water process. The ethanol and isopropanol processes show a significantly higher energy demand. The operating entrainer flow rate hints at the performance of the entrainer recovery column because it defines the load of this column. Ethanol and water display a relatively low entrainer-to-process feed ratio of less than one. Chlorobenzene needs an entrainer-to-process feed ratio of 1.615, whereas the isopropanol process requires a ratio of 2.742. Although until now only one column has been analyzed, it can already be concluded that, based on these observations, it is extremely unlikely that using isopropanol as entrainer is a good choice because this process requires both the highest energy cost in the extractive column and the largest entrainer-to-process feed ratio. The comparison of the ethanol, water, and isopropanol processes is not that easy because the energy requirement of the

extractive column and the operating entrainer flow rate lead to contradicting conclusions.

With the design of the extractive column, the entrainer flow rate and thus the mass balance for the complete flowsheet have been fixed. Assuming a fixed entrainer composition $\mathbf{x}_E$, the form of the problem statement allows decoupling of both separation steps and design of each column separately without any loss of information. Therefore, the entrainer recovery column can now be analyzed in the second design step. For the determination of the minimum energy demand of this column, the standard rectification body method (Bausa et al., 1998) is used. The results are shown in Table 2. It can be seen that the chlorobenzene process loses the advantage of having the lowest energy demand in the extractive column by needing a significantly higher amount of energy in the entrainer recovery column than that of the water process. The overall energy demand of the process alternatives indicates that the chlorobenzene and the water process have nearly identical energy demands and therefore operating costs. Unless a decision can be made based on plant-specific considerations or the chemical hazard of the entrainer, a further, more rigorous analysis by simulation is needed. The results for the shortcut analysis can be directly used as a starting point for this simulation case study. Ethanol and isopropanol, however, can be deleted from the list of candidate entrainers. This result conforms with that obtained by Laroche et al. (1991).

Conclusions

A new design method for extractive distillation processes, where the separation is limited by minimum-boiling azeotropes, has been developed. It is based on the nonlinear analysis of pinch maps and an extension of the rectification body method for the determination of the minimum energy demand. The method is general and can be applied to arbitrary azeotropic mixtures without limitations regarding the number of components or certain types of splits.

The method determines the minimum entrainer flow rate and the corresponding feasible reflux ratio as the thermodynamic boundaries of the extractive distillation process. Using the concept of operational constraints, the method further aids in finding robust operating conditions. The calculation of the minimum and maximum reflux ratios provides the range of feasible reflux policies and therefore contributes a measurement of process flexibility.

Using the shortcut design procedure, the complete extractive distillation process, consisting of extractive column and solvent recovery, can easily be analyzed. Assuming a fixed entrainer composition $\mathbf{x}_E$ the form of the problem statement allows the decoupling of both separation steps and the design of each column separately without any loss of information. This represents a big advantage over simulation-based approaches where both the simulation of each single column and their coupling are time-consuming and often cause numerical problems. If the entrainer composition $\mathbf{x}_E$ is not known in advance, it offers additional degrees of freedom that are available for optimization. This optimization balances the required purity of the recycle stream vs. the desired product purities. Allowing a limited amount of impurities in the entrainer recycle stream will usually lead to energy savings with respect to the entrainer recovery column. However, the impurities will then almost completely appear in the distillate product of the extractive column. Therefore, such optimization will be useful only in cases where significant impurity of the product streams is tolerable. In most industrial processes high-purity products will be required and therefore the allowable range of impurity of the entrainer recycle stream will be narrow. Doherty and Malone (2001) report that typical recycle purities will be around 99.95 mol %.

Table 2. Reboiler Heat Duties for the Extractive Distillation of a Binary Acetone–Methanol Mixture with Different Entrainers

	Reboiler Heat Duty $Q_{B,min}/F$ (10^7 kJ/kmol)		
Entrainer	Extractive Column	Recovery Column	Total
Chlorobenzene	4.730	3.871	8.601
Water	6.769	1.858	8.627
Ethanol	11.347	5.685	17.032
Isopropanol	14.650	9.509	24.159

The extension of this process scheme with a preconcentration column or any additional upstream or downstream unit is straightforward. Also the entrainer recovery system is not required to be a single simple column but can be substituted by a more complex arrangement. It can even be replaced by any other unit operation or a hybrid unit, provided that there is a suitable design method for this unit. An upcoming publication will deal with such process alternatives and also discuss the separation of a four-component mixture by extractive distillation in one complex column.

Sometimes extractive columns with two or more feed streams are also used for separations within a distillation region where both product compositions are located on a connecting residue curve. In this case the extractive effect is not necessary to overcome a limitation imposed by azeotropy. According to the theory of distillation regions, such separations are always feasible for large reflux ratios regardless of the distribution of the feed streams. Therefore, a minimum entrainer flow rate enabling feasible operation of the column does not exist. However, the introduction of a second feed stream may save a significant amount of energy. Although such processes have not been the focus of this contribution it should be noted that the generalization of the rectification body method for columns with two streams can directly be used for this class of processes.

Acknowledgments

This research was partially supported by the Deutsche Forschungsgemeinschaft. The authors thank their colleague M. Mönnigmann for many fruitful discussions on nonlinear analysis.

Notation

B = bottom product flow rate, kmol/s
C = number of components
D = distillate product flow rate, kmol/s
E = entrainer feed flow rate, kmol/s
F = process feed flow rate, kmol/s
h = molar enthalpy, J/kmol
L = liquid flow rate, kmol/s
N = section product flow rate, kmol/s
p = pressure, bar
Q = energy, W

r = reflux ratio
T = temperature, K
u_i = state variable
V = vapor flow rate, kmol/s
$\mathbf{x}$ = vector of vapor phase compositions $\mathbf{x} = [x_1, \ldots, x_C]^T$
x_i = liquid-phase composition of component i
$\mathbf{y}$ = vector of vapor phase compositions $\mathbf{y} = [y_1, \ldots, y_C]^T$
y_i = vapor-phase composition of component i
α, β = design constraints
φ_i = design variable

Subscripts

bif = from bifurcation analysis
B = bottom
D = distillate
E = entrainer
lo = lower bound
max = maximum
min = minimum
N = section product
n = tray number
op = operational
P = propanol
r = reflux ratio
up = upper bound
W = water

Superscripts

L = liquid phase
V = vapor phase
vap = vaporization

Literature Cited

Andersen, H. W., L. Laroche, and M. Morari, "Effect of Design on the Operation of Homogeneous Azeotropic Distillation," *Comp. Chem. Eng.*, **19**(1), 105 (1995).

Bauer, M. H., and J. Stichlmair, "Design and Economic Optimization of Azeotropic Distillation Processes Using Mixed-Integer Nonlinear Programming," *Comp. Chem. Eng.*, **22**(9), 1271 (1998).

Bausa, J., "Näherungsverfahren für den konzeptionellen Entwurf und die thermodynamische Analyse von destillativen Trennprozessen," Reihe 3, Nr. 692, Fortschritt-Berichte VDI, Düsseldorf (2001).

Bausa, J., and W. Marquardt, "Shortcut Design Methods for Hybrid Membrane/Distillation Processes for the Separation of Nonideal Multicomponent Mixtures," *Ind. Eng. Chem. Res.*, **39**(6), 1658 (2000).

Bausa, J., R. v. Watzdorf, and W. Marquardt, "Shortcut Methods for Nonideal Multicomponent Distillation: 1. Simple Columns," *AIChE J.*, **44**(10), 2181 (1998).

Beyn, W.-J., A. Champneys, E. Doedel, W. Govaerts, Y. A. Kuznetsov, and B. Sanstede, "Numerical Continuation and Computation of Normal Forms," *Handbooks of Dynamical Systems*, B. Fiedler, ed., Vol. 2, pp. 149–219 (2002).

Black, C., "Distillation Modeling of Ethanol Recovery and Dehydration Processes for Ethanol and Gasohol," *Chem. Eng. Prog.*, **76**, 78 (1980).

Doherty, M. F., and G. A. Caldarola, "Design and Synthesis of Homogeneous Azeotropic Distillations: 3. The Sequencing of Columns for Azeotropic and Extractive Distillations," *Ind. Eng. Chem. Fundam.*, **24**, 474 (1985).

Doherty, M. F., and M. F. Malone, *Conceptual Design of Distillation Systems*, McGraw-Hill, New York (2001).

Doherty, M. F., and J. D. Perkins, "On the Dynamics of Distillation Processes—I. The Simple Distillation of Multicomponent Non-reacting, Homogeneous Liquid Mixtures," *Ind. Eng. Chem. Proc. Des. Dev.*, **17**, 272 (1978).

Fidkowski, Z. T., M. F. Doherty, and M. F. Malone, "Feasibility of Separations for Distillation of Nonideal Ternary Mixtures," *AIChE J.*, **39**(8), 1303 (1993).

Foucher, E. R., M. F. Doherty, and M. F. Malone, "Automatic Screening of Entrainers for Homogeneous Azeotropic Distillation," *Ind. Eng. Chem. Res.*, **30**, 760 (1991).

Franklin, N. L., and J. S. Forsyth, "The Interpretation of Minimum Reflux Conditions in Multi-Component Distillation," *Trans. Inst. Chem. Eng.*, **31**, 363 (1953).

Harper, P. M., R. Gani, P. Kolar, and T. Ishikawa, "Computer-aided Molecular Design with Combined Molecular Modeling and Group Contribution," *Fluid Phase Equilibria*, **158–160**, 337 (1999).

Julka, V., and M. F. Doherty, "Geometric Behavior and Minimum Flows for Nonideal Multicomponent Distillation," *Chem. Eng. Sci.*, **45**(7), 1801 (1990).

Knapp, J. P., and M. F. Doherty, "Minimum Entrainer Flows for Extractive Distillation: A Bifurcation Theoretic Approach," *AIChE J.*, **40**(2), 243 (1994).

Knight, J. R., and M. F. Doherty, "Optimal Design and Synthesis of Homogeneous Azeotropic Distillation Sequences," *Ind. Eng. Chem. Res.*, **28**, 564 (1989).

Köhler, J., P. Aguirre, and E. Blass, "Minimum Reflux Calculations for Nonideal Mixtures Using the Reversible Distillation Model," *Chem. Eng. Sci.*, **46**(12), 3007 (1991).

Laroche, L., N. Bekiaris, H. W. Andersen, and M. Morari, "Homogeneous Azeotropic Distillation: Comparing Entrainers," *Can. J. Chem. Eng.*, **69**, 1302 (1991).

Laroche, L., N. Bekiaris, H. W. Andersen, and M. Morari, "The Curious Behavior of Homogeneous Azeotropic Distillation—Implications for Entrainer Selection," *AIChE J.*, **38**(9), 1309 (1992).

Levy, S. G., and M. F. Doherty, "Design and Synthesis of Homogeneous Azeotropic Distillations: 4. Minimum Reflux Calculations for Multiple-Feed Columns," *Ind. Eng. Chem. Fundam.*, **25**, 269 (1986).

Pham, H. N., P. J. Ryan, and M. F. Doherty, "Design and Minimum Reflux for Heterogeneous Azeotropic Distillation Columns," *AIChE J.*, **35**, 1585 (1989).

Thong, D. Y.-C., F. J. L. Castillo, and G. P. Towler, "Destillation Design and Retrofit Using Stage-composition Lines," *Chem. Eng. Sci.*, **55**, 625 (2000).

Underwood, A. J., "Fractional Distillation of Multicomponent Mixtures," *Chem. Eng. Prog.*, **44**, 603 (1948).

Urdaneta, R. Y., J. Bausa, S. Brüggemann, and W. Marquardt, "Analysis and Conceptual Design of Ternary Heterogeneous Distillation Processes," *Ind. Eng. Chem. Res.*, **41**, 3849 (2002).

Appendix A: Analysis of the Acetone–Methanol–Water Separation

The analysis of the acetone–methanol–water (AMW) separation shows an interesting behavior of the saddle-node bifurcation branch that was already mentioned in the section dealing with the calculation of $(E/F)_{min,bif}$ and is discussed here in more detail. In contrast to the PWG example, where a ternary branching point was found on this line, the saddle-node bifurcation branch of the AMW example approaches the binary acetone–methanol edge without displaying any local maxima or minima (see Figure A1). The plot of the reflux ratio r on the saddle-node bifurcation branch shows a constant decrease of r if E/F is increased. When reaching the binary edge, the saddle-node bifurcation branch branches itself at $E/F = 0.806$. The ternary branch leaves the composition space. The additional branch runs on the binary acetone–methanol edge toward the pure component vertices (see Figure A1). Following the binary branch toward the acetone vertex, the entrainer feed flow rate of the saddle-node bifurcation decreases until a minimum is reached at $E/F = 0.740$. From there on, E/F increases along the path. According to the rules obtained from nonlinear analysis of the pinch maps, this minimum marks the topological lower bound for the entrainer feed flow rate. The behavior of the azeotrope pinch branch in Figure A1 (left) supports this claim. Therefore, it is necessary to consider *all* branches of saddle-node bifurcation originating from the azeotrope pinch branch to correctly determine this bound.

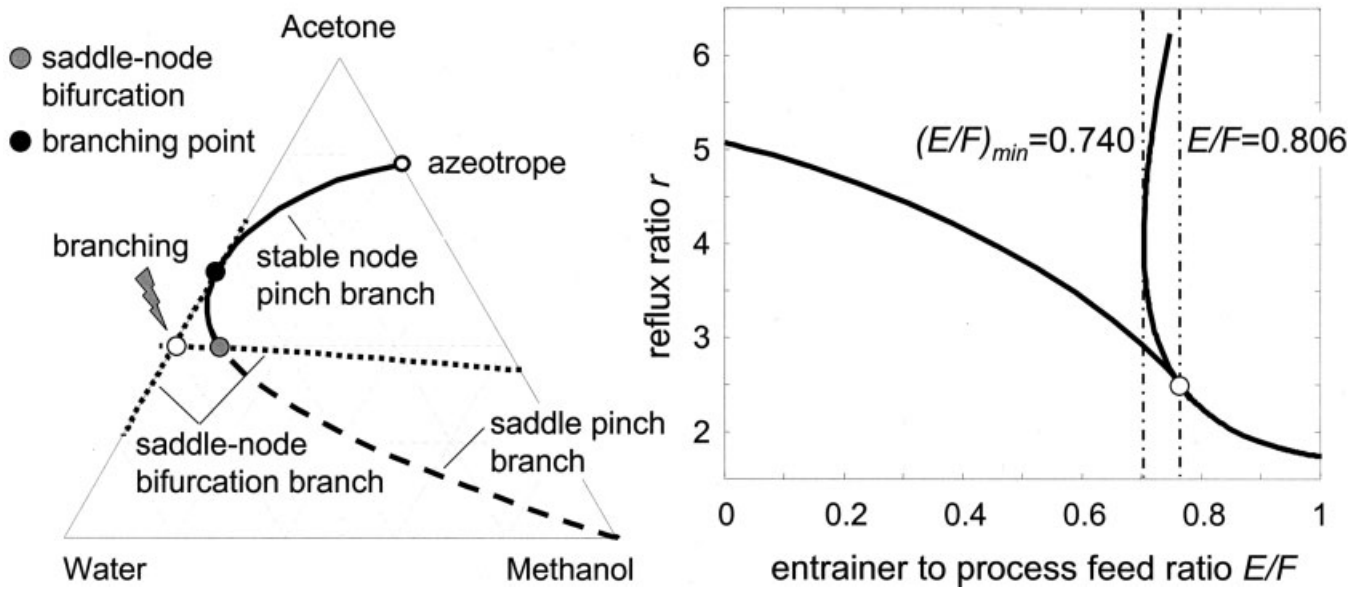

Figure A1. Left: Pinch branches (solid, dashed) at $E/F = 0.740$ and loci of saddle-node bifurcation (dotted) for the AMW separation.

Note that some pinch branches on the binary acetone–water edge have been omitted for better legibility of the saddle-node bifurcation lines. Right: Reflux ratio on the saddle-node bifurcation lines as a function of the entrainer to process feed ratio.

Appendix B: Analysis of the Acetone–Methanol–Chlorobenzene Separation

As mentioned in the section dealing with the determination of the minimum entrainer flow rate E_{min}, the acetone–methanol–chlorobenzene (AMC) separation requires a minimum entrainer feed ratio $(E/F)_{min} = 1.173$, which is much larger than its topological lower bound of $(E/F)_{min,bif} = 0.788$. This behavior is in contrast with the other separation examples discussed in this article, which are all characterized by $E_{min} \approx E_{min,bif}$, and is discussed here in more detail.

Figure B1 shows the pinch map in a ternary diagram and the reflux ratio on the pinch branches at $(E/F)_{min,bif}$. Note the characteristic ternary branching point (pitchfork bifurcation) at $r = 11.53$. We now apply the criteria for topological feasibility of the separation. The first rule is that there should be no ternary unstable node pinch on the pinch branch originating

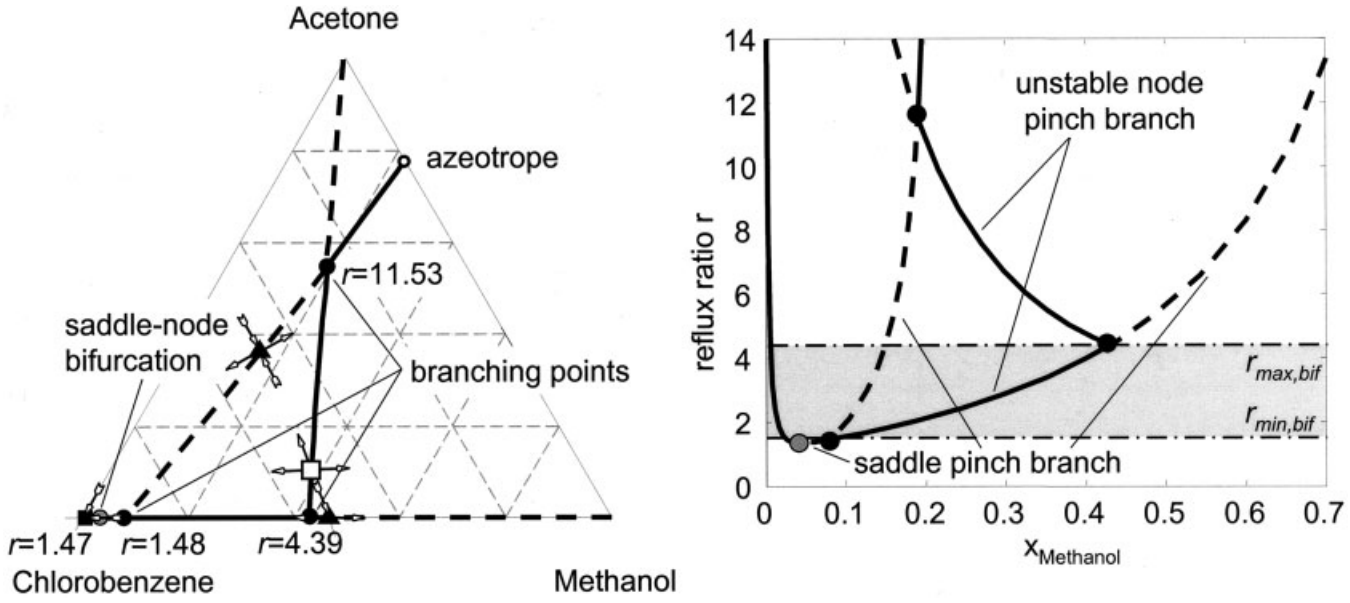

Figure B1. Pinch branches (solid, dashed) at $E/F = 0.788$ and pinch points at $r_{max,bif} = 5.0$ for the AMC separation (left).

Reflux ratio along the pinch branches (right).

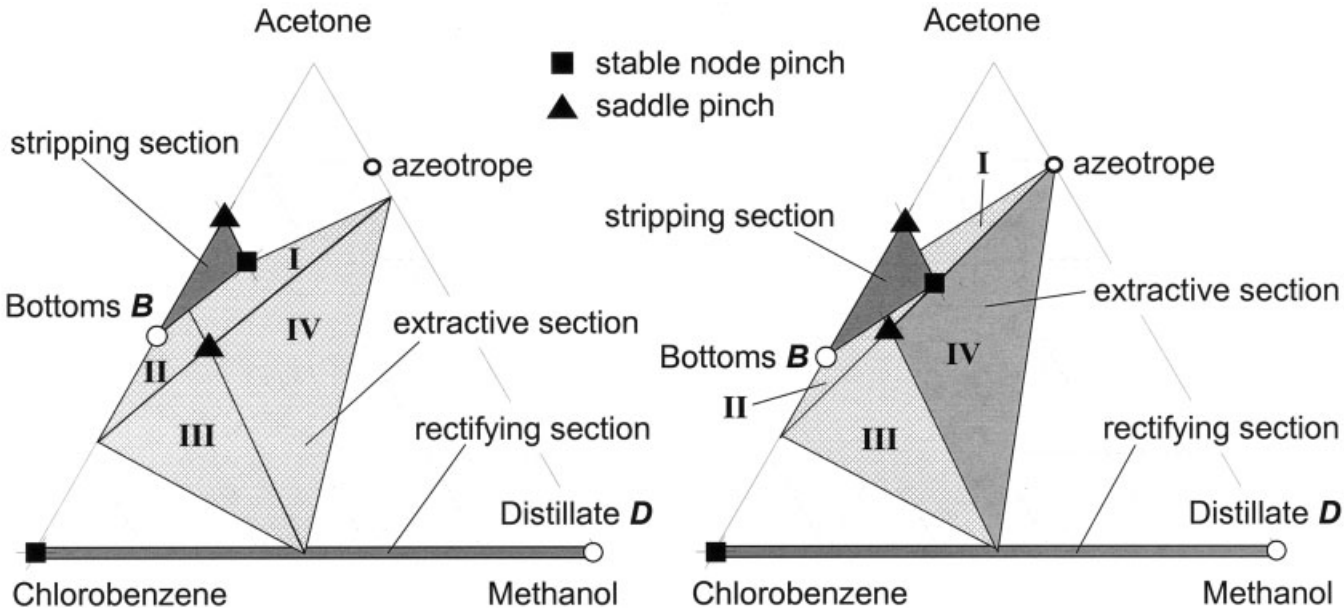

Figure B2. Rectification bodies at $E/F = 1.0$ and $r_{max,bif} = 6.196$ (left) and at $(E/F)_{min} = 1.173$ and $r_{max,bif} = 7.640$ (right).

from the azeotrope. It can be seen that this is case for any reflux ratio below $r_{max,bif} = 4.39$, where this pinch branch branches with the binary methanol–chlorobenzene edge. The second rule requires the existence of a ternary saddle pinch on a pinch branch originating either at the acetone or methanol vertex. Following the pinch branch originating at the acetone vertex, it can be seen that such ternary saddle pinch is obtained for any reflux ratio above $r_{min,bif} = 1.48$, where the pinch branch branches with the binary methanol–chlorobenzene edge.

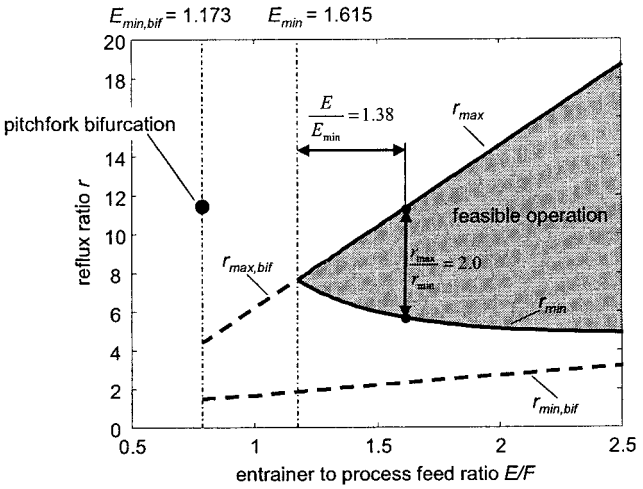

Figure B3. Minimum and maximum reflux ratios for the AMC separation as a function of the entrainer feed flow rate.

Hence, at $(E/F)_{min,bif}$, a finite range of topologically feasible reflux ratios $1.48 \leq r \leq 4.39$ exists, whereas the PWG example (cf. Figure 8) is characterized by an infinitely small range $r_{min,bif} = r_{max,bif}$ for $(E/F)_{min,bif}$. The absence of a finite range of reflux ratios in the PWG example is caused by the formation of two ternary saddle-node bifurcation points on the water pinch branch for $E/F > (E/F)_{min,bif}$. Such saddle-node bifurcation points do not exist for the AMC example.

In contrast to the PWG separation (cf. Figure 15) the rectification bodies of the AMC column do not intersect at $(E/F)_{min,bif}$ and $r_{max,bif}$. In fact, even for a significantly larger entrainer-to-feed ratio $E/F = 1.0$, the bodies do not intersect at $r_{max,bif} = 6.196$, as can be seen from Figure B2 (left). The first entrainer feed ratio for which the bodies intersect at $r_{max,bif}$ is $E/F = 1.173$ (see Figure B2, right). Therefore, this value for E/F corresponds to the minimum entrainer feed ratio $(E/F)_{min}$.

The feasible region of operation of the AMC example is shown in Figure B3. Analogously to the PWG separation (cf. Figure 16), the feasible region of the AMC mixture is bounded by the minimum entrainer feed ratio $(E/F)_{min}$ and the upper and lower reflux ratios r_{max} and r_{min}, respectively. The range of feasible reflux ratios increases with increasing E/F. Because of the characteristics of the pinch map of the AMC mixture discussed above some differences between Figures B3 and 16 can be seen, for example, the finite range of feasible reflux ratios $r_{min,bif} \leq r \leq r_{max,bif}$ at $(E/F)_{min}$ and the location of the pitchfork bifurcation. However, it is important to note that the different behavior of the mixtures does not pose a problem to the general applicability of the new design method.

Manuscript received Mar. 11, 2003, and revision received Aug. 11, 2003.